UNIVERSIDADE DE LISBOA

FACULDADE DE FARMÁCIA

Bioactive terpenoids from *Euphorbia pubescens*: isolation and derivatization

João Paulo Magalhães Carréu

Dissertation supervised by Professor Noélia Maria da Silva Dias Duarte and co-supervised by Professor Maria José Umbelino Ferreira

Master's in Medicinal and Biopharmaceutical Chemistry

2020

UNIVERSIDADE DE LISBOA

FACULDADE DE FARMÁCIA

Bioactive terpenoids from *Euphorbia pubescens*: isolation and derivatization

João Paulo Magalhães Carréu

Dissertation supervised by Professor Noélia Maria da Silva Dias Duarte and co-supervised by Professor Maria José Umbelino Ferreira

Master's in Medicinal and Biopharmaceutical Chemistry

2020

This thesis was conducted at the Natural Products Chemistry group, Research Institute for Medicines (iMed.ULisboa), Faculty of Pharmacy, University of Lisbon.

The financial support was provided by Fundação para a Ciência e Tecnologia (FCT, Portugal (Project PTDC/MED-QUI/30591/2017).

Acknowledgments

Firstly, I would like to thank and express my most sincere gratitude to Professor Noélia Duarte, not only for supervising all of my work and guiding me, but also for her patience and friendliness towards me, and for encouraging me to always go the extra mile on my work.

I would also like to express my gratitude to Professor Maria José Umbelino for her guidance, for sharing all the experience she has so I could improve my work and for her constant support.

I sincerely acknowledge Fundação para a Ciência e Tecnologia for (Project PTDC/MED-QUI/30591/2017) and Portuguese Mass Spectrometry Network (Rede Nacional de Espectrometria de Massa – RNEM; LISBOA-01-0145-FEDER-402-022125)

I would like to thank my laboratory partners, namely David Cardoso, Joana Rita and Shirley Sancha for all their constant help, support and for making the workspace such a wonderful one.

I want to take the opportunity to thank my course colleagues and friends, Andreia Alexandra, Marta Valente, Raquel Durão, Raquel Mestre and Sofia Milheiro, for their friendship, helpfulness and support.

To my Discord friends, I thank them for almost ten years of companionship and support, and for helping me maintain my focus and helping me relax when I needed it most.

A special thank you to my girlfriend, Ana Fonseca, for her companionship and love, for sharing her knowledge and experience, and most important of all, for always being by my side.

I am deeply thankful to my family, especially my sister Rute, my grandmother Otília and my uncle Jorge for a lifetime of love and support.

Lastly, but the most important, I am uttermost grateful to my parents, Natalina and José, for their unconditional love, patience and support, for always encouraging me to go further, for always believing in me, and for the sacrifices they made to provide me with the education and the opportunities to reach where I am today.

Abstract

Euphorbia species have been used in traditional medicine to treat cancer, tumors and warts. In the last decades, considerable attention has been focused on plants from this genus as a source of biologically active compounds (e.g. antitumor, cytotoxic, antibacterial and antiviral). These plants are characterized for biosynthesizing macrocyclic and polycyclic diterpenes, as well as triterpenes, steroids and phenols. In particular, the discovery of macrocyclic jatrophane- and lathyrane-type diterpenes as a new class of potent modulators of the transmembrane protein P-gp (P-glycoprotein), the main ABC transporter involved in multidrug resistance in cancer, has fostered an increasing interest in the research of this genus.

To find out new bioactive compounds, the phytochemical study of three fractions of *Euphorbia pubescens* methanol extract was performed using chromatographic techniques, such as column chromatography or preparative thin layer chromatography.

Overall, eleven compounds were isolated, including euphopubescenol, a jatrophane-type macrocyclic diterpene, three *ent*-abietane diterpenic lactones (helioscopinolides A, B and E) five pentacyclic triterpenes (taraxerone, taraxerol, taraxerol acetate; isomultiflorenol and isomultiflorenyl acetate), one steroid (β-sitosterol), and one phenolic compound (coniferaldehyde). Taraxerone was isolated in major amounts. Therefore, taking advantage of the ketone function at C-3, molecular derivatization reactions were attempted, namely condensation of taraxerone with hydrazine monohydrate, phenylhydrazine and 2,4-dinitrophenylhydrazine to obtain three new hydrazone derivatives. The structures of all compounds, including stereochemical features, were deduced from their physical and spectroscopic data, which included: infrared spectroscopy, mass spectrometry (MS), and extensive one- and two- dimensional nuclear magnetic resonance studies (COSY, HMQC and HMBC), and by comparison of these data with those reported in the literature.

Further studies will be performed in order access their ability as P-gp modulators.

Keywords: *Euphorbia pubescens*, multidrug resistance, pentacyclic triterpenes, diterpenes.

Resumo

As espécies do género *Euphorbia* têm sido utilizadas na medicina tradicional, desde a Antiguidade, para o tratamento de verrugas, tumores, cancros e infeções intestinais, entre outras patologias.

Nas últimas décadas, o estudo fitoquímico destas espécies tem merecido uma especial atenção, devido ao isolamento de um enorme número de compostos biologicamente ativos, dos quais se destacam os diterpenos policíclicos e macrocíclicos, com esqueletos do tipo jatrofano e latirano, triterpenos tetracíclicos e pentacíclicos e esteroides. Das diversas atividades biológicas demonstradas por estes compostos, são de salientar os resultados obtidos com os diterpenos macrocíclicos, que revelaram uma importante atividade moduladora da glicoproteína-P, uma das principais proteínas transmembranares envolvidas na multirresistência das células tumorais aos fármacos anti-neoplásicos.

Esta dissertação teve como principal objetivo a pesquisa de novos compostos bioativos a partir de *Euphorbia pubescens*. Para tal, foram utilizadas duas abordagens: i) o isolamento de compostos a partir três frações do extrato metanólico; ii) derivatização molecular de compostos isolados em maior quantidade. O estudo fitoquímico foi realizado recorrendo a técnicas cromatográficas, nomeadamente cromatografia em coluna ou cromatografia preparativa em camada fina.

Foram isolados e identificados onze compostos, incluindo cinco triterpenos pentacíclicos (taraxerona, taraxerol, acetato de taraxerol, isomultiflorenol e acetato de isomultiflorenol), um diterpeno macrocíclico do tipo jatrofano (euphopubescenol), três lactonas diterpénicas do tipo *ent*-abietano (helioscopinolidos A, B e E), um esteroide (β-sitosterol) e um composto fenólico (coniferaldeído).

A taraxerona foi isolada em maiores quantidades, pelo que se procedeu à derivatização da função cetona em C-3 por condensação com a hidrazina, fenil-hidrazina e a 2,4-dinitrofenilhidrazina, obtendo-se três novos derivados.

As estruturas químicas dos compostos foram deduzidas com base nas suas características físicas e espectroscópicas (IV, espectrometria de massa, ressonância magnética nuclear unidimensional - ^{1}H-RMN e ^{13}C-RMN - e bidimensional - ^{1}H-^{1}H-COSY, HMQC, HMBC) e por comparação com dados descritos na literatura.

Futuramente, serão realizados estudos adicionais que permitirão avaliar a capacidade dos compostos obtidos como moduladores da glicoproteína-P em células tumorais resistentes.

Palavras-chave: *Euphorbia pubescens*, multiresistência, triterpenos pentacíclicos, diterpenos

Index

Tables

Figures

Schemes

Abbreviations and Symbols

^{1}H-NMR	^{1}H Nuclear Magnetic Resonance
^{13}C-NMR	^{13}C Nuclear Magnetic Resonance
AcAc-CoA	Acetoacetyl-Coenzyme A
Acetyl-CoA	Acetyl-Coenzyme A
ATP	Adenosine Triphosphate
ABC	ATP Binding Cassette
Bz	Benzoyl
δ	Chemical Shift
CC	Column Chromatography
COSY	Correlation Spectroscopy
J	Coupling Constant
d	Doublet
dd	Doublet of Doublet
ddd	Doublet of Doublet of Doublet
DEPT	Distortionless Enhancement by Polarization Transfer
DMAPP	Dimethylallyl diphosphate
dt	Doublet of Triplets
ESI-MS	Electrospray Ionization Mass Spectrometry
HMBC	Heteronuclear Multiple Bond Correlation
HMG-CoA	S-3-hydroxy-3-methylglutaryl-CoA
HMGR	S-3-hydroxy-3-methylglutaryl reductase
HMQC	Heteronuclear Multiple-Quantum Correlation
IR	Infrared
IPP	Isopentenyl diphosphate
ispC	1-deoxy-D-xylulose-5-phosphate reductoisomerase
ispD	4-diphosphocytidyl-2-C-methyl-Derythritol synthase
ispE	4-diphosphocytidyl-2-C-methyl-Derythritol kinase
ispF	2-C-methyl-D-erythritol 2,4-cyclodiphosphate synthase
ispG	4-Hydroxy-3-methyl-but-2-enyl diphosphate synthase
ispH	4-Hydroxy-3-methyl-but-2-enyl diphosphate reductase
m.p.	Melting point

MEP	Methylerythritol Phosphate Pathway
MVD	Mevalonate diphosphate decarboxylase
MK	Mevalonate kinase
MVA	Mevalonate pathway
MDR	Multidrug resistance
m	Multiplet
NMR	Nuclear Magnetic Resonance
P-gp	P-glycoprotein
ppm	Parts per million
PMK	Phosphomevalonate kinase
$[M+H]^+$	Protonated Molecule Ion
q	Quadruplet
m/z	Ratio of mass to charge
s	Singlet
t	Triplet
TLC	Thin Layer Chromatography
UV	Ultraviolet

Introduction

1.1 *Euphorbia pubescens*

Euphorbia pubescens Vahl, also known as *Euphorbia hirsuta* L., is an erect perennial herb, up to 1 meter in height and possessing yellowish green flowers (Figure 1). This plant is native to the Mediterranean Region and was introduced in Mexico, Canary Islands and South Africa.[1][2][3]

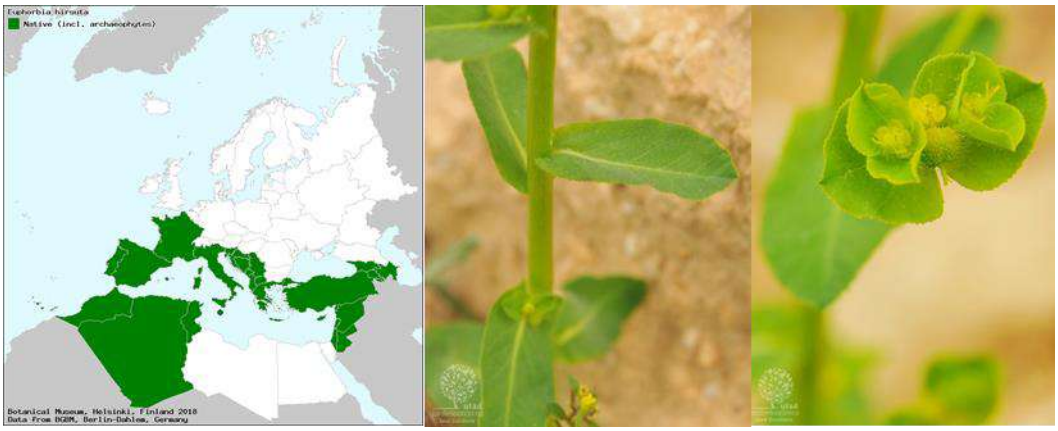

***Figure 1** - From left to right: Native distribution of Euphorbia pubescens, stem and leaves of the plant; and flowers and leaves of the plant.[2][3]*

The Euphorbiaceae is one of the largest and more diverse families amongst angiosperms, ranging from large trees to small weeds, distributed all over the world. Consensus on the number of species in this family has not yet been achieved, with some authors reporting that it has more than 2000 species and others claiming that it has more than 8000 species in 300 genera (1,2).

Euphorbia species have been used as medicinal plants since ancient times for the treatment of various ailments, such as tumors and warts (3). For example, in Nigeria, *Euphorbia hirta* is used by the major tribes for the treatment of asthma, with the plant being squeezed into water and then the extract is drunk by the patient (4). *Euphorbia kansui* has been traditionally used in the Far East for the treatment of edema, asthma and various other diseases, and is now under studies for the prevention and treatment of psoriasis(5).

Another example of the therapeutical potential of this genus is *Euphorbia neriifolia*, which is used in traditional medicine as an effective treatment for rheumatism, sciatica, gout

[1] http://ww2.bgbm.org/EuroPlusMed/PTaxonDetail.asp?NameCache=Euphorbia%20hirsuta
[2] http://www.worldfloraonline.org/taxon/wfo-0000962564
[3] https://jb.utad.pt/especie/Euphorbia_hirsuta

and bronchitis. It is under several studies, in which anti-inflammatory, analgesic, immune-modulation, hepato-protection, antioxidant, diuretic, and anti-viral/tumoral/bacterial activities have shown the most promising results (6). A biopolymeric fraction named BET, isolated from *Euphorbia tirucalli*, has also been shown to be an auspicious therapeutic agent in the treatment of arthritis through the modulation of the host's immune response (7).

More importantly, there is the example of Picato®, an ingenol mebutate (Figure 2) gel for the treatment of actinic keratosis, a skin lesion usually caused by sun exposure that can, sometimes, evolve into squamous cell carcinoma. In comparison to the market options at the time, this gel offered a treatment with shorter duration of use with a favorable side-effect profile in which the lesions healed faster. Ingenol mebutate is a diterpenic compound found in *Euphorbia peplus*, treating the lesions of this condition by inducing cell death and is also able of inhibiting tumor cell growth.

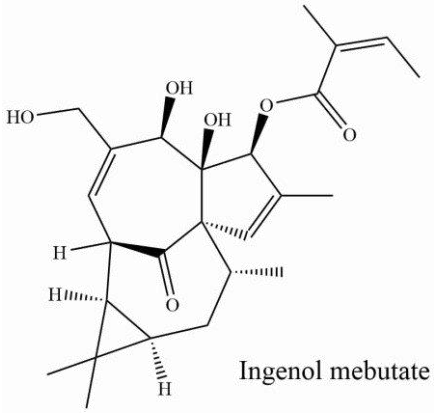

Figure 2 *- Structure of ingenol mebutate (Picato®).*

1.2 Main constituents of *Euphorbia* species: triterpenes and diterpenes

Triterpenes and diterpenes are major constituents found in *Euphorbia* genus. Terpenoids, also known as terpenes or isoprenoids, are a large group of structurally diverse natural products that comprises at least 40.000 compounds. The terpenic skeletons are derived from two isoprene units (C_5 building blocks, Scheme 1), the isopentenyl diphosphate (IPP) and its isomer dimethylallyl diphosphate (DMAPP). As shown in Scheme 1, depending on the number of isoprene units (C_5 building blocks) they can be classified as monoterpenes (C_{10}), sesquiterpenes (C_{15}), diterpenes (C_{20}), sesterterpenes (C_{25}), triterpenes (C_{30}) and tetraterpenes (C_{40})(8,9).

Terpenoids have fundamental functions, such as growth, development, reproduction and defense; as well as a more specialized role in the plants, originating from immense divergent

gene evolution, such as stress response, pollinator attraction or even repellent activity. In human society, this specialization has been profitable, as terpenoids are used as flavors, fragrances, insecticides, pharmaceuticals and as raw industry materials for adhesives or coatings.

The isoprene units (IPP and DMAPP) are biosynthesized in plants by two different pathways: the mevalonate (MVA) pathway and the methylerythritol phosphate (MEP) pathway (Scheme 2)(8).

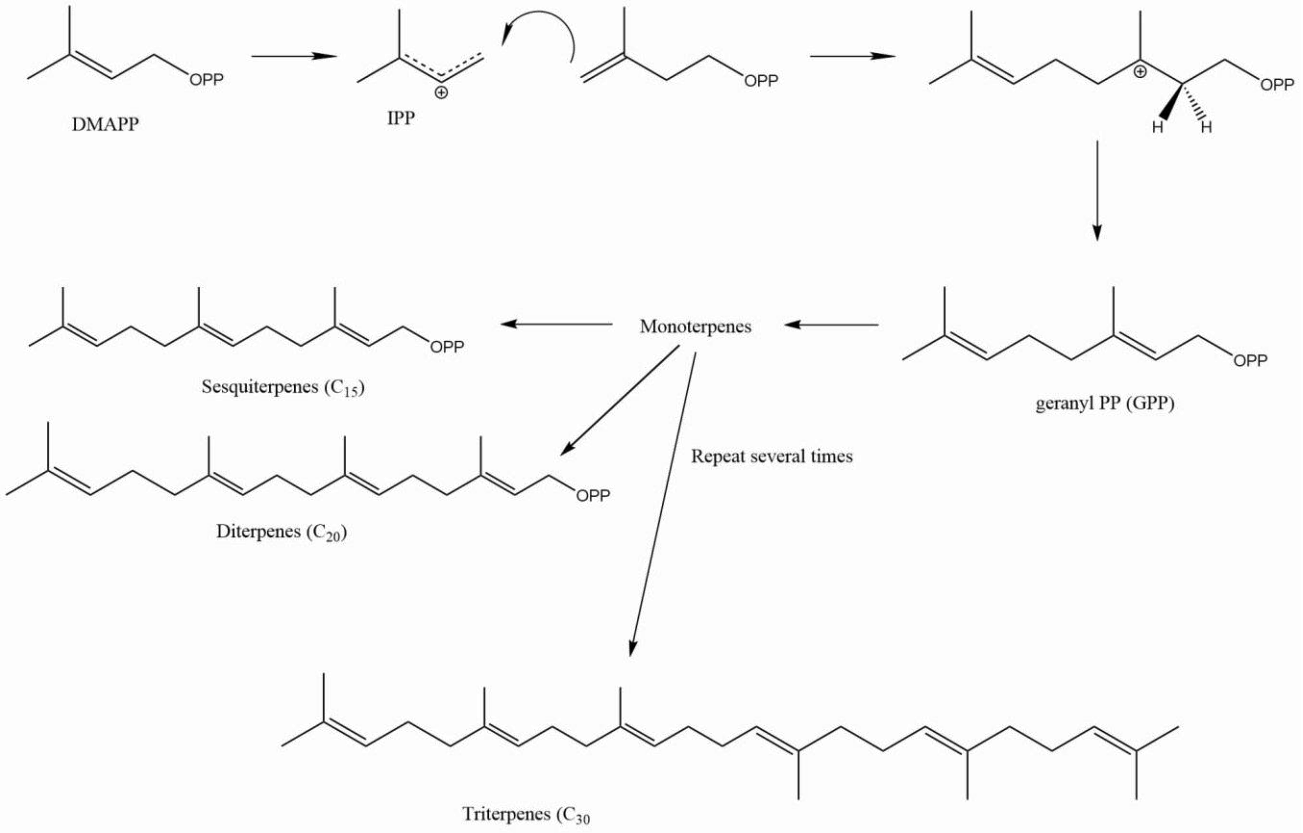

Scheme 1 *- Formation of terpenes from DMAPP and IPP.*

The mevalonate pathway (MVA, Scheme 2) starts with Claisen condensation of two molecules of acetyl-CoA to yield acetoacetyl-CoA (AcAc-CoA) that further reacts with another molecule of acetyl-CoA, forming S-3-hydroxy-3-methylglutaryl-CoA (HMG-CoA). S-HMG-CoA is then converted to R-mevalonate through the catalyst HMG-CoA reductase (HMGR), and sequentially being converted into IPP and DMAPP through phosphorylation catalyzed by mevalonate kinase (MK) and phosphomevalonate kinase (PMK) and an ATP-driven decarboxylative elimination catalyzed by mevalonate diphosphate decarboxylase (MVD)(8–10).

The methylerythritol phosphate (MEP, Scheme 2) pathway, also known as mevalonate-independent pathway and deoxyxylulose phosphate pathway, was one of the greatest

discoveries regarding plant terpenoid biosynthesis (9,11). This pathway begins with a condensation of pyruvate and D-Glyceraldehyde-3-phosphate (GAP), catalyzed by DXP synthase, forming 1-deoxy-D-xylulose-5-phosphate (DXP), which is then converted into 2-C-methyl-D-erythritol-4-phosphate (MEP) by IspC. MEP is then converted into 4-diphosphocytidyl-2C-methyl-erythritol (CDP-ME) by the enzyme IspD, and CDP-ME suffers phosphorylation by IspE, leading to the formation of 4-diphosphocytidyl-2C-methyl-D-erythritol-2-phosphate (CDP-ME2P). CDP-ME2P is cyclized by IspF into 2C-methyl-D-erythritol-2,4-cyclodiphosphate (MEcPP) which then suffers a two-electron reduction by IspG and is converted into a mixture of IPP and DMAPP by IspH. (8,12).

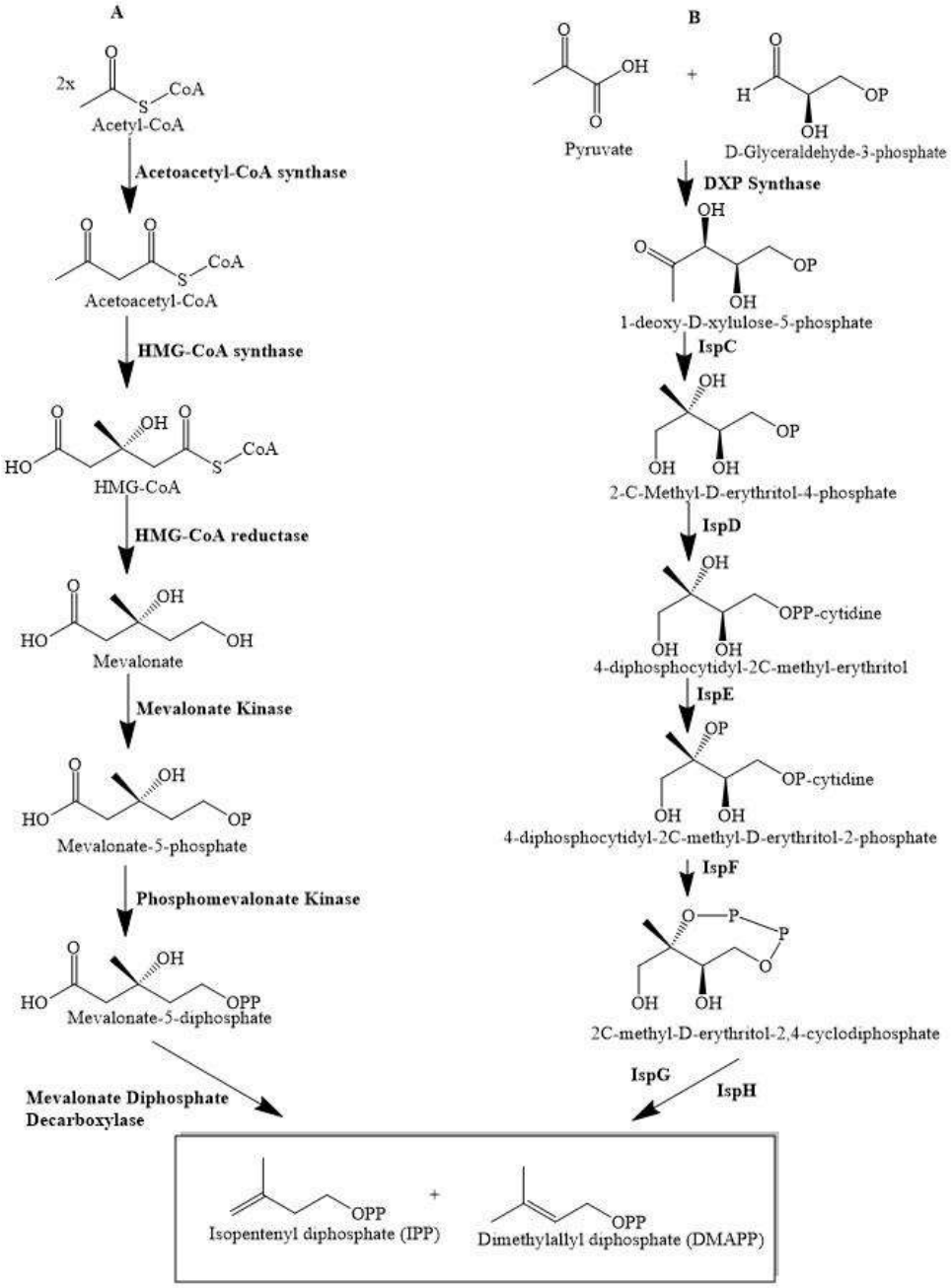

Scheme 2 *- Terpenoid pathways, A being the MVA pathway and B being the MEP pathway (adapted from (5,6)).*

Isopentenyl diphosphate (IPP) is transformed into dimethylallyl diphosphate (DMAPP) by the enzyme isopentenyl-isomerase (IPP isomerase) (Scheme 1). A molecule of DMAPP is condensed with a molecule of IPP to obtain geranyl diphosphate (GPP) and the addition of another molecule of IPP originates farnesyl diphosphate (FPP). If one more IPP is added, geranylgeranyl diphosphate (GGPP) is obtained, while a sequential addition leads to geranyl farnesyl diphosphate (GFPP). GPP is the precursor of monoterpenes (C_{10}), FPP of sesquiterpenes (C_{15}), GGPP of diterpenes (C_{20}) and GFPP of sesterterpenes (C_{25}).

A reductive tail-to-tail dimerization of two molecules of FPP, catalyzed by a membrane-bound enzyme, leads to squalene, which is the precursor of triterpenes and steroids. All-*trans*-squalene is the immediate precursor of all cyclic triterpenoids.

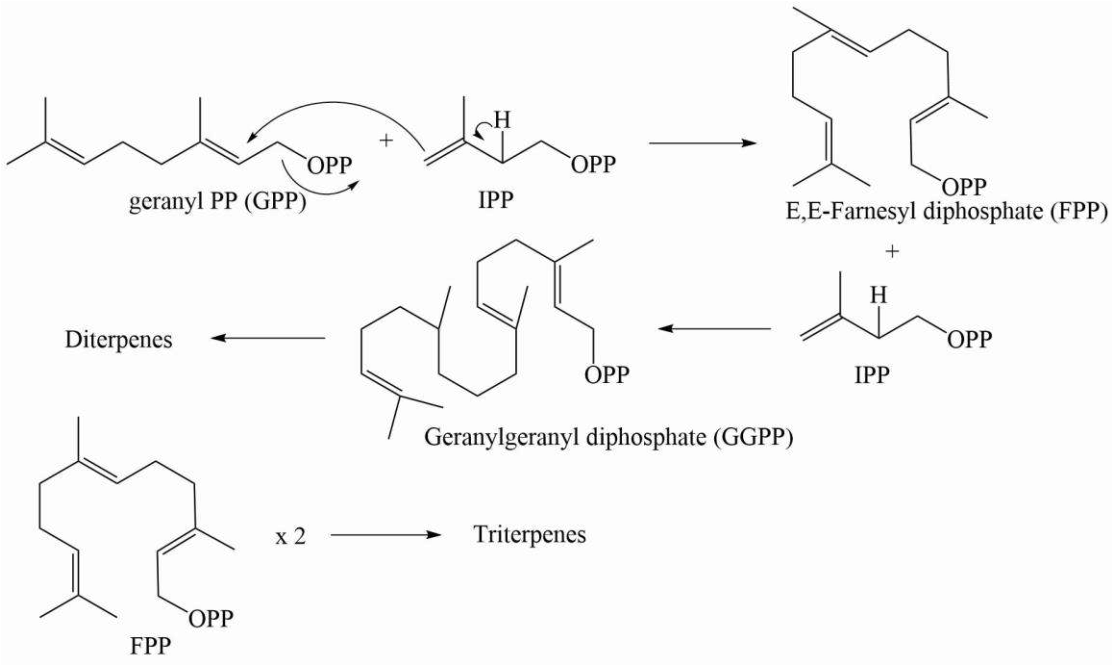

Scheme 3 *- General scheme of the formation of diterpenes and triterpenes.*

In this section, a literature review of the new triterpenes and diterpenes isolated from *Euphorbia* sp. between 2015 and 2019 are presented, as well as their respective biological activities, focusing on cytotoxic and antiproliferative activities (Tables 1 – 2 and Figure 3). This timeframe was chosen due to the fact that a previous work about these compounds and this *Euphorbia* species already presented a literature review until 2015 (13). This review was conducted on Google Scholar and PubMed, using the keywords "*Euphorbia* terpenes", "*Euphorbia* diterpenes", "*Euphorbia* triterpenes" and "*Euphorbia pubescens*", with the year filter from 2015 to 2019.

Table 1 *- Triterpenes isolated from Euphorbia sp. and their respective activity*

Euphorbia **Species**	**Triterpene (Structure number)**	**Biological Activity**	**Reference**
Euphorbia helioscopia	Euphorbatrine A (**1**)	Compounds **1-7** increase cell death in Hela and HT-29 cell lines.	(14)
	Euphorbatrine B (**2**)		
	Euphorbatrine C (**3**)		
	Euphorbatrine D (**4**)		
	Euphorbatrine E (**5**)		
	Euphorbatrine F (**6**)		
	Euphorbatrine G (**7**)		
Euphorbia pedroi	Spiropedroxodiol (**8**)	Compound **8** demonstrated to be a very strong MDR reversal agent in both L5178Y-MDR and Colo320 cell lines.	(15)
Euphorbia schimperi C. Presl	Cycloschimperols A (**9**)	Compounds **9** and **10** showed significant cytotoxic activity against MCF-7, HepG2, and HCT-116 cells lines.	(16)
	Cycloschimperols B (**10**)		
Euphorbia pterococca Brot.	Cycloartenyl-2′*E*,4′*E*-decadienoate (**11**)	Compound **11** showed exhibited moderate but significant inhibitory effects on α/β-hydrolase 12.	(17)
	Cycloartenyl-2′*E*,4′*Z*-decadienoate (**12**)		
	24-methylenecycloartanyl-2′*E*,4′*Z*-tetradecadienoate (**13**)		
	24-oxo-29-norcycloartanyl-2′*E*,4′*Z*-hexadecadienoate (**14**)		
Euphorbia alatavica Boiss	Alatavolide (**15**)	Compounds **15** and **16** showed weak and moderate cytotoxicity, respectively, against Hela, MCF-7 and A549 cell lines.	(18)
	Alatavoic acid (**16**)		

Table 1 *- Triterpenes isolated from Euphorbia sp. and their respective activity (cont.)*

Euphorbia boissierana Prokh.	3-[(O-β-D-fucopyranosy l-(1→2)-β-D-glucopyranosyl)oxy]lup-20(29)-en-3β,28-diol (**17**)		(19)
Euphorbia resinifera Berg	Euphorol A (**18**)	Compounds **18** to **26** exhibited various degrees of cytotoxic effect against MCF-7, U937 and C6 cancer cell lines.	(20)
	Euphorol B (**19**)		
	Euphorol C (**20**)		
	Euphorol D (2**1**)		
	Euphorol E (**22**)		
	Euphorol F (**23**)		
	Euphorol G (**24**)		
	Euphorol H (**25**)		
	Euphorol I (**26**)		
	Euphorol K (**27**)	Compounds **27** and **28** exhibited cytotoxic activity against MCF-7, U937 and C6 cancer cell lines.	(21)
	Euphorol J (**28**)		
Euphorbia tirucalli L.	Euphorol L (**29**)		(22)
	Euphorol M (**30**)		
	Euphorol N (**31**)		

Table 2 *- Diterpenes isolated from Euphorbia sp. and their respective activity*

***Euphorbia* Species**	**Diterpenes (Structure number)**	**Biological Activity**	**Reference**
Euphorbia stracheyi Boiss	*nt*-Kaurane-16*β*,17,19-triol-3-one (**32**)		(23)
Euphorbia neriifolia	Euphorantin S (**33**)	Compound **38** demonstrated moderate anti-HIV-1 activity.	(24)
	Euphorantin T (**34**)		
	Euphorneroid A (**35**)		
	Euphorneroid B (**36**)		

***Table 2** - Diterpenes isolated from Euphorbia sp. and their respective activity (cont.)*

	Euphorneroid C (37)		
	Euphorneroid D (**38**)		
Euphorbia lathyris	*Euphorbia* factor L_{27} (**39**)	Compound **40** showed antiproliferative activity against MCF-7, MDA-MB-468, 786-0 and HepG2 human cancer cell lines.	(25)
	Euphorbia factor L_{28} (**40**)		
Euphorbia laurifolia	15β-Acetoxy-7β-nicotinoyloxy-3β,8α-di-(2-methylpropanoyloxy)-4αH,9αH,11αH-lathyra-5*E*,12*E*-dien-14-one (**41**)		(26)
	2-*Epi*-latazienone (**42**)		
Euphorbia ebracteolata	Euphoroid A (**43**)	Compounds **44** and **45** demonstrated cytotoxic activity against human cancer cell lines A549, MCF-7, Mewo, SH-SY5Y, Lovo, and HepG2.	(27)
	Euphoroid B (**44**)		
	Euphoroid C (**45**)		
	Ebractenoid O (**46**)	Compounds **46-48** exhibited anti-inflammatory activities, by inhibition of LPS-induced NO production *in vitro* in macrophages.	(28)
	Ebractenoid P (**47**)		
	Ebractenoid Q (**48**)		
Euphorbia clementei Boiss	4,20-dideoxy-4*α*-phorbol-12β-acetate-13*α*-isobutyrate (**49**)	Compound **49** exhibited a weak selective cytotoxic activity against HL60 cell line.	(29)
Euphorbia fischeriana Steud	Euphorin E (**50**)	Compounds **50-58** inhibited mammosphere (a clump of mammary gland cells) formation in MCF-7 cells.	(30)
	Euphorin H (**51**)		
	Yuexiandajisu E (**52**)		
	ent-3β-hydroxyatis-16-ene-2,14-dione (**53**)		
	19-O-β-D-glucopyranosyl-*ent*-atis-16-ene-3,14-dione (**54**)		
	Euphorin C (**55**)		

***Table 2** - Diterpenes isolated from Euphorbia sp. and their respective activity (cont.)*

	Ebractenoid C (56)		
	Ebractenoid F (**57**)		
	Jolkinol A (**58**)		
Euphorbia kansui	kansuinin P (**59**)		(31)
	kansuinin Q (**60**)		
Euphorbia yinshanica	*Ent*-3α,16-dihydroxylabda-8(17),12(E),14-triene (**61**)		(32)
	Ent-14(S),15-dihydroxylabda-8(17)-12(E)-dien-18-oic acid (**62**)		
Euphorbia pithyusa	3β,7β,13β,17-O-Tetraacetyl-5α-O-benzoyl-14-oxopremyrsinol (**63**)	Compound **68** exhibited good inhibitory activity against CHIKV replication on Vero cells, while compounds **63**-**67** and **69** exhibited weak inhibitory activity.	(33)
	3β,7β,15β,17-O-Tetraacetyl-5α-O-benzoyl-14-oxopremyrsinol (**64**)		
	3β,7β,13β,17-O-Tetraacetyl-5α-O-(2-methylbutyryl)-14-oxopremyrsinol (**65**)		
	7β,13β,17-O-Triacetyl-5α-O-(2-methylbutyryl)-3β-O-propanoyl-14-oxopremyrsinol (**66**)		
	7β,17-O-Diacetyl-5α-O-benzoyl-13β-nicotinyl-		

***Table 2** - Diterpenes isolated from Euphorbia sp. and their respective activity (cont.)*

	3β-O-propanoyl-14-oxopremyrsinol (**67**)		
	13β,17-O-Diacetyl-5α-O-benzoyl-7β-hydroxy-3β-O-propanoyl-14-oxopremyrsinol (**68**)		
	5α,7β-O-Diacetyl-14β-O-benzoyl-3β-O-propanoylmyrsinol (**69**)		
Euphorbia welwitschii	Euphowelwitschines A (**70**)	Compounds **72** and **73** showed antiproliferative selectivity toward the resistant gastric cell line EPG85-257RDB, with **73** having an MDR-selective antiproliferative effect on pancreatic (EPP-181) human cell lines.	(34)
	Euphowelwitschines B (**71**)		
	Welwitschene (**72**)		
	Epoxywelwitschene (**73**)		
Euphorbia resinifera Berg	Euphoresin A (**74**)	Compounds **74** and **75** exhibited small cytotoxic activities against MCF-7, U937, and C6 cancer cell lines.	(35)
	Euphoresin B (**75**)		
Euphorbia thymifolia	(2*R*, 3*S*, 5*S*, 9*S*, 10*R*)-2,3-dihydroxy-*ent*-abieta-8(14),12(13)-dien-7-one (**76**)		(36)
Euphorbia dracunculoides Lam	4-deoxy-4(β)H-8-hydroperoxyphorbol-12-benzoate-13-isobutyrate (**77**)		(37)
Euphorbia guyoniana	Guyonianin G (**78**)	Compounds **78** and **79** showed strong activity as inhibitors of GIRK current, showing promise in the development of antiarrhythmic drugs.	(38)
	Guyonianin H (**79**)		

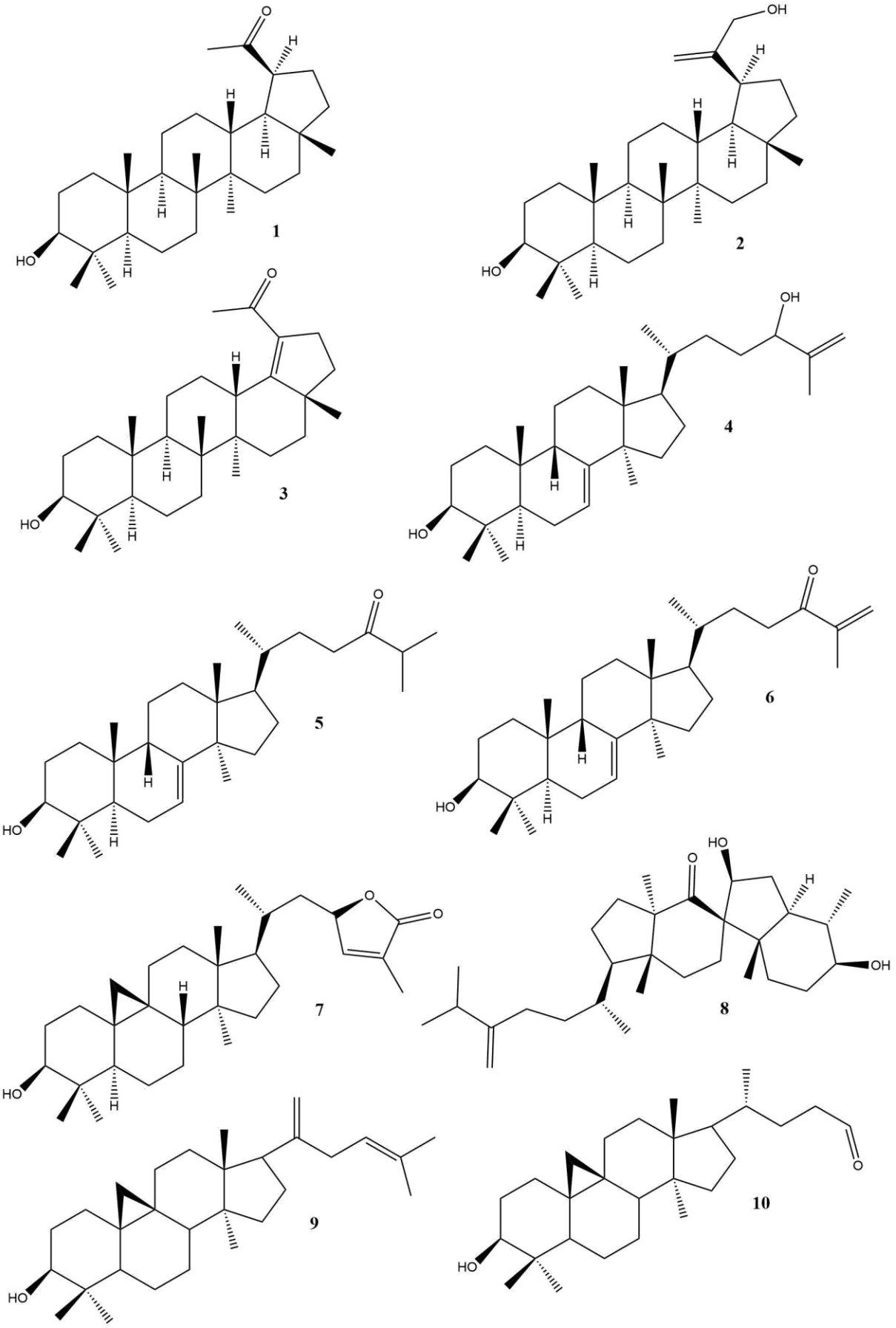

Figure 3 *- Structures of compounds from Tables 1 and 2.*

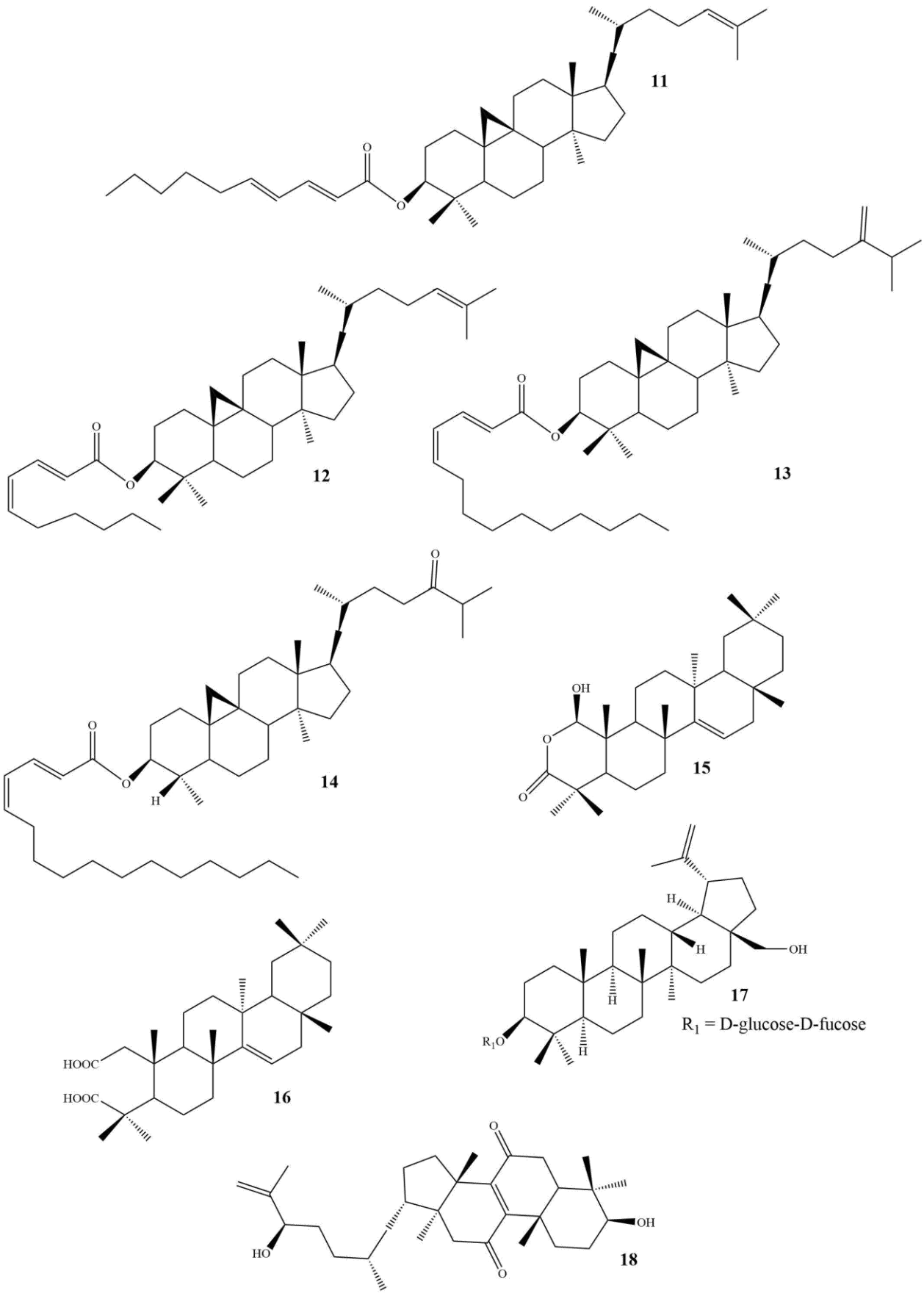

Figure 3 *- Structures of compounds from Tables 1 and 2 (cont.)*

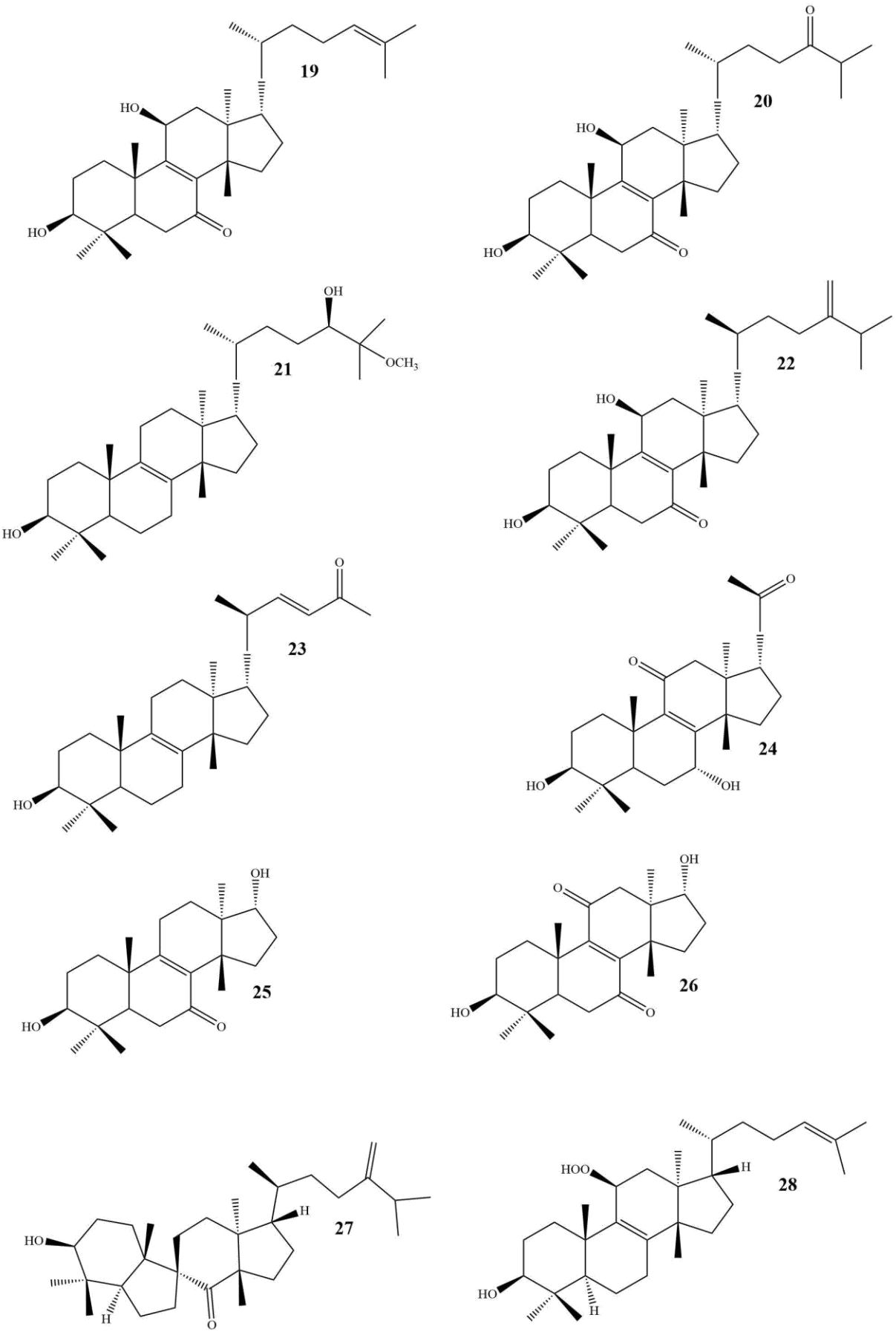

Figure 3 *- Structures of compounds from Tables 1 and 2 (cont.)*

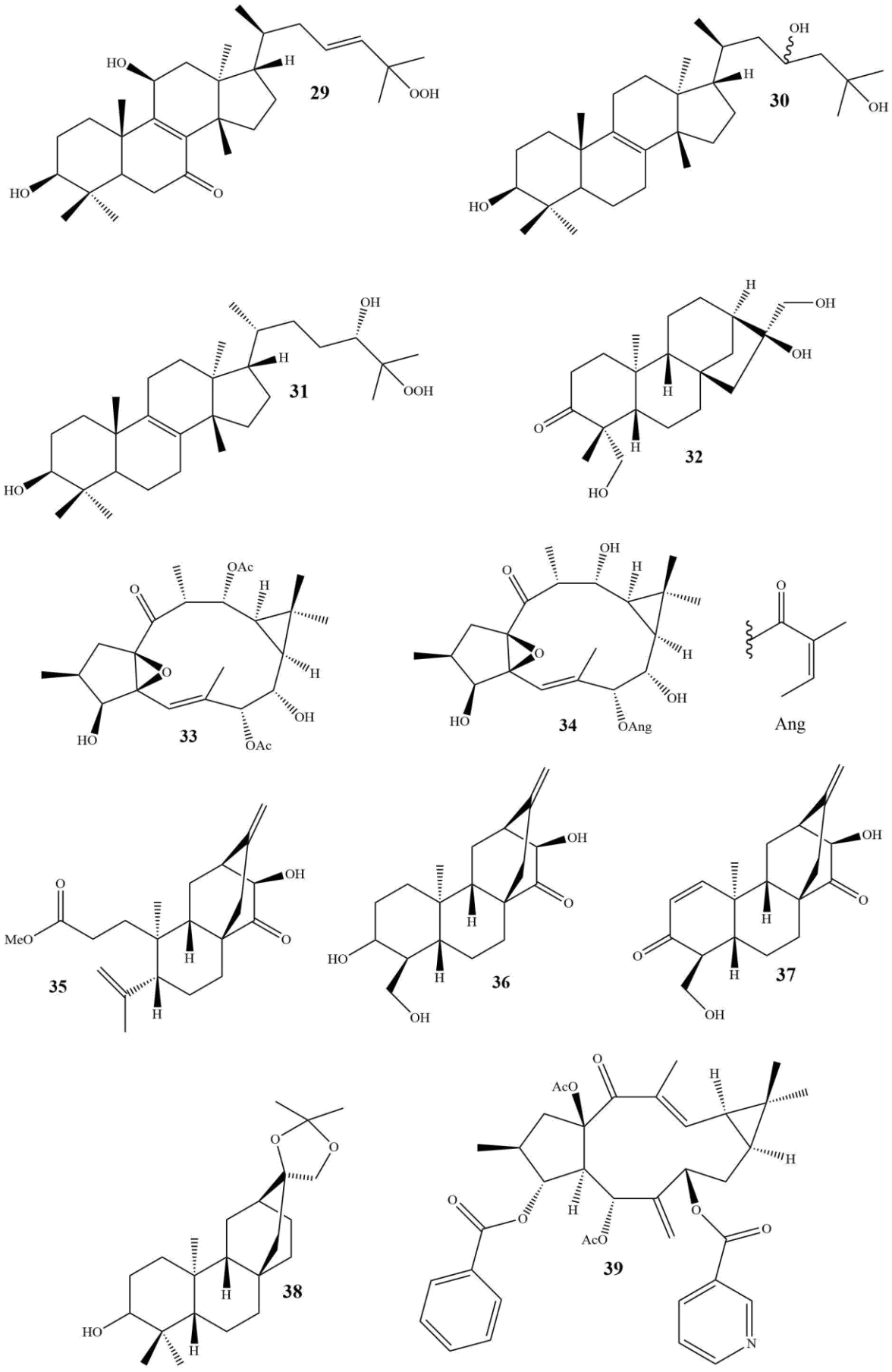

Figure 3 *- Structures of compounds from Tables 1 and 2 (cont.)*

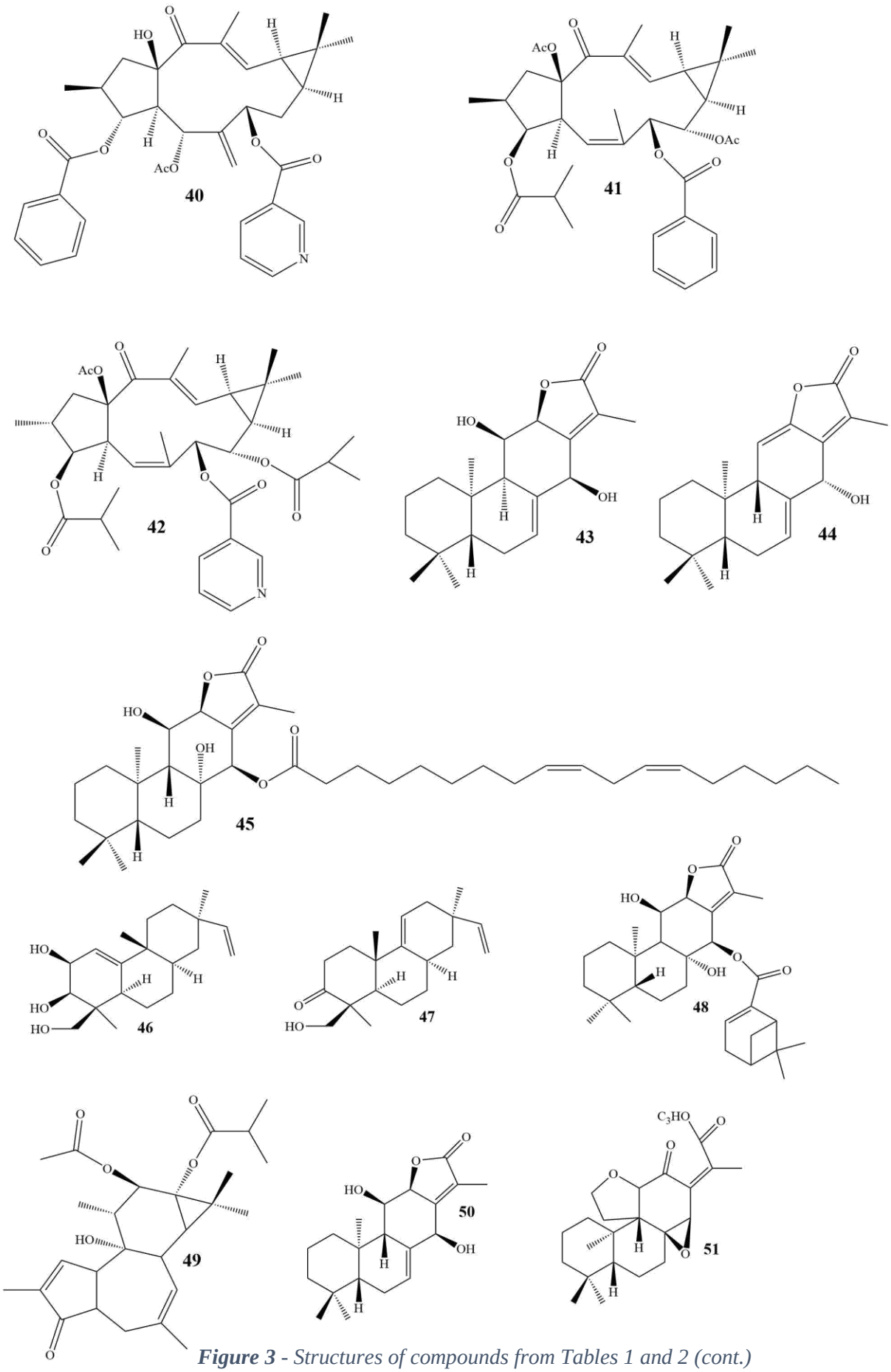

Figure 3 *- Structures of compounds from Tables 1 and 2 (cont.)*

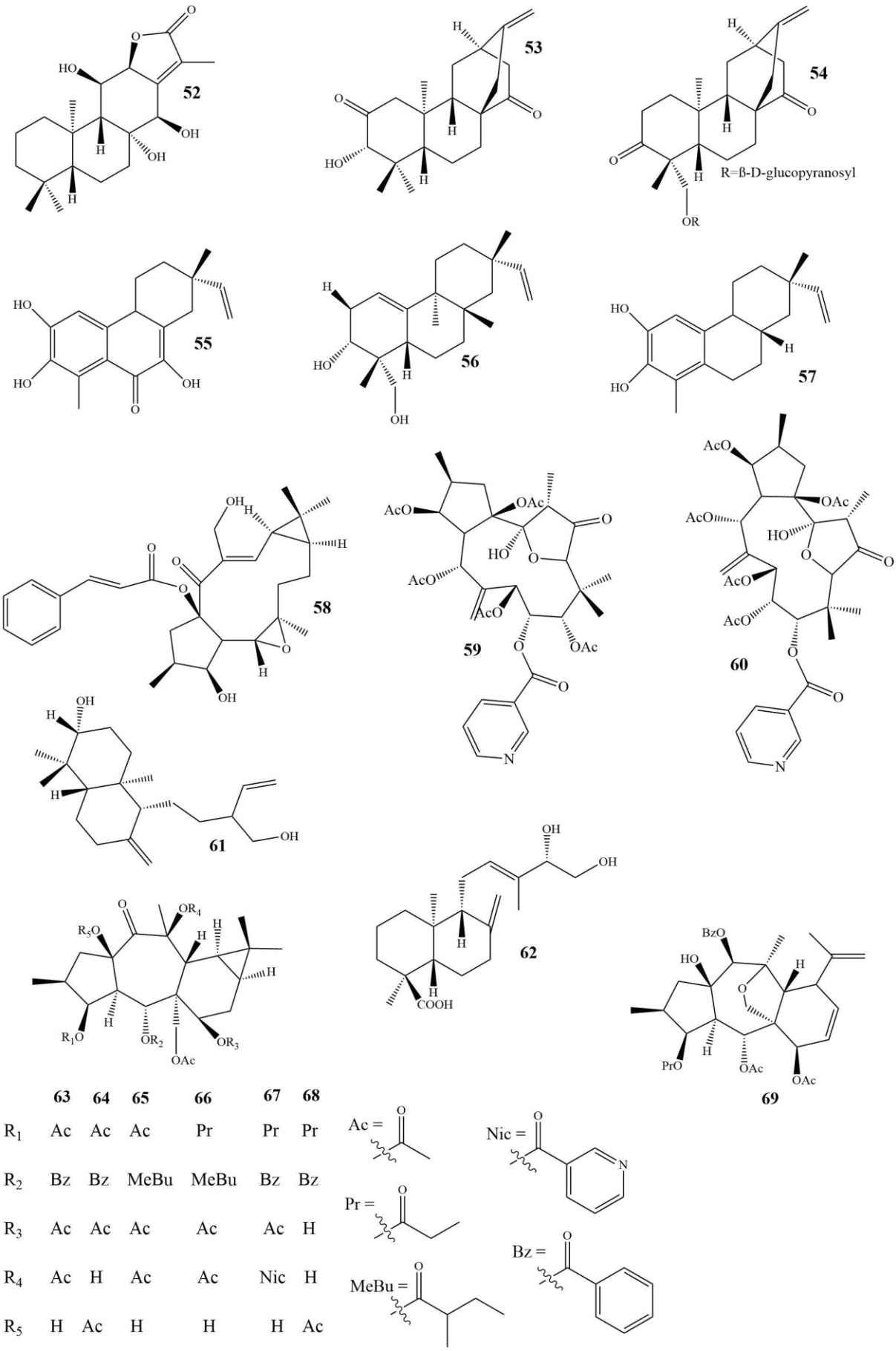

Figure 3 *- Structures of compounds from Tables 1 and 2 (cont.)*

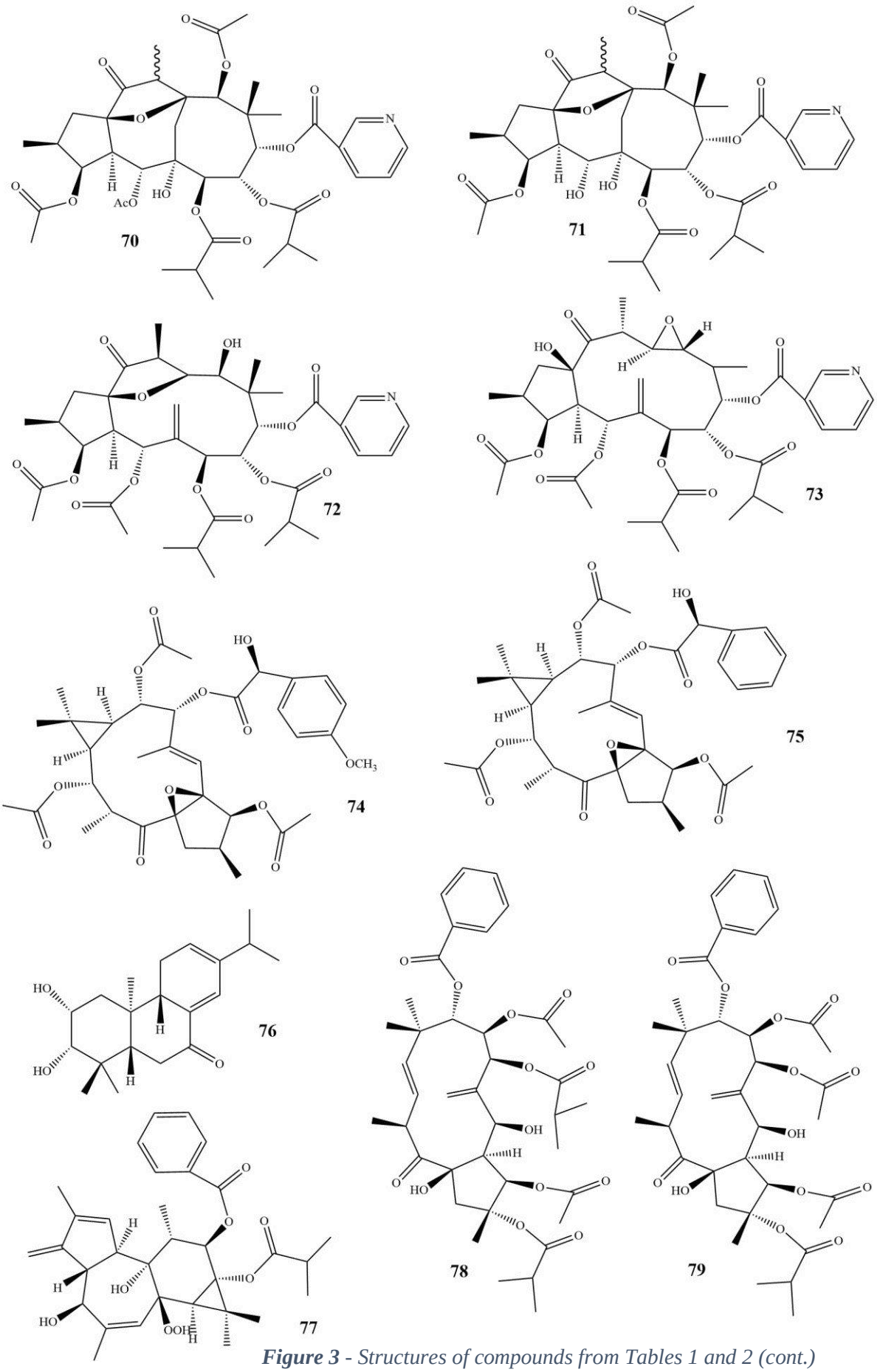

Figure 3 *- Structures of compounds from Tables 1 and 2 (cont.)*

1.3 Multidrug resistance in cancer

Cancer is one of the most concerning health threats, being responsible for 21% of all mortalities worldwide and 9.1% in developing countries in 2013 (38). In 2018 it is estimated that 18.1 million new cases of cancer appeared and caused 9.6 million deaths, with statistics saying that 1 in 5 men and 1 in 6 women worldwide developing cancer in their lifetime (39). One of the major obstacles in cancer treatment is multidrug resistance (MDR).

MDR happens when cancer cells present a phenotype that is cross resistant against multiple unrelated drugs that are different, both structurally and functionally, posing a serious health issue (40). MDR can be divided into two types: intrinsic, occurring due to the various genetic characteristics of cells, possibly being present at diagnosis and with cancer cells not responding to standard chemotherapy drugs from the beginning; and acquired, that occurs due to genetic alterations that follow chemotherapy (38,41). Successful treatment of patients is impaired due to the widespread of this phenomenon and, since MDR can include various drugs, from hormones and antibiotics to immunosuppressive agents, MDR inhibitors have become compounds of interest (42).

A common cause of MDR is the increased levels of certain ATP-binding cassette (ABC) transporters in the cell membranes (43). One of these transporters, P-gp (P-glycoprotein), can be blocked by a group of compounds called MDR modulators. Several studies showed that they may enhance the pharmacological treatment when combined with an anticancer drug, by competing with the cytotoxic agent for binding to the active site of membrane transporters and thus reducing drug efflux (44–46). Some of these compounds, like verapamil or cyclosporin A, failed in clinical trials (Figure 3). They belong to the 1st-generation P-gp modulators, which normally are associated with toxicity, lack of specificity and require high doses to be effective. The 2nd-generation modulators, such as valspodar and dexverapamil, which, despite being better than the 1st generations in every point described before, suffer from unwanted interactions with other transport proteins. The 3rd-generation modulators, of which tariquidar and laniquidar are examples, showed high specificity, low toxicity and high potency, and yet have no notable drug interactions with common chemotherapy compounds, however they also failed in clinical trials (Figure 4) (42).

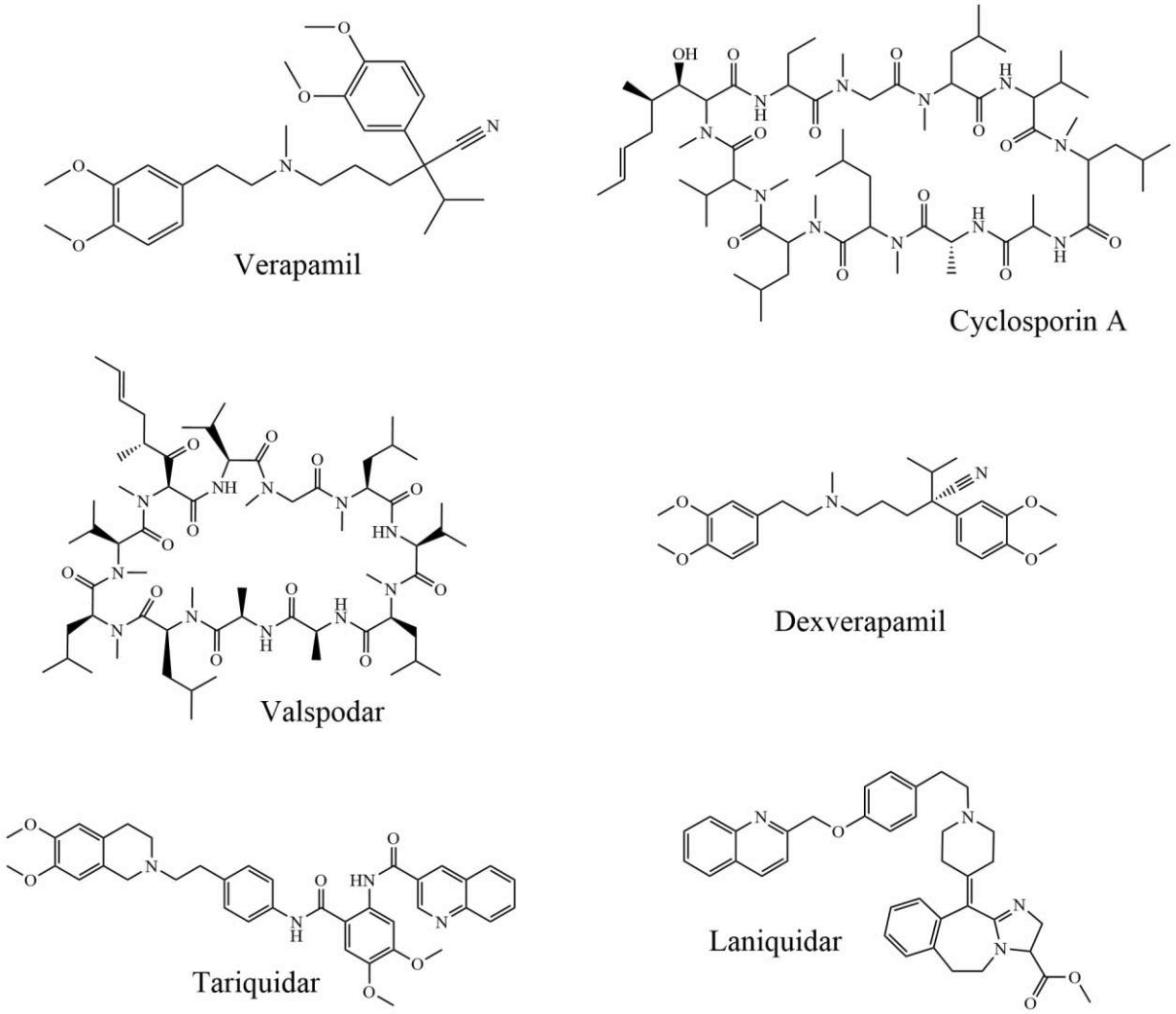

Figure 4 *- Examples of 1st (Verapamil and Cyclosporin A), 2nd (Valspodar and Dexverapamil) and 3rd generation (Tariquidar and Laniquidar) MDR modulators.*

1.4 The future of 4th generation modulators

Despite several issues, natural products have a great potential for bringing new drugs to the market (47). In the last decade, over 70% of ABC transporter inhibitors reported were either natural products or their respective secondary metabolites, therefore these natural-derived compounds were designated as fourth generation, due to the relevance of these natural sources in finding increasingly ideal ABC inhibitors (46). Natural products are investigated for their low toxicity and selective, but potent, behavior, so plants, marine organisms and fungi have been the main sources for compounds such as flavonoids, coumarins, diterpenes, amongst others (43).

Yet, sometimes analogues of the original compound are needed, as can be seen in the example of fumitremorgin C (Figure 5), a fungal toxin that is a very efficient ABCG2 inhibitor, but displays high neurotoxicity, whereas the analogue generated displays higher potency and selectivity, but less toxicity (45). Another example is found in *Desmodium styracifolium* (Fabaceae), a plant that may have an effect in drug metabolism, particularly P-gp. This activity can be attributed to its contents, like flavonoids/isoflavonoids, alkaloids and triterpenoids, that possess one or more phenolic hydroxyl groups, that, under physiological conditions, can dissociate partly, forming phenolate ions that could interact unselectively with enzymes, possibly leading to protein inactivation (48).

Spiropedroxodiol (Figure 5), a novel compound isolated from *Euphorbia pedroi*, was evaluated for its MDR reversal activity on resistant human colon adenocarcinoma cells (Colo320) and human ABCB1 gene transfected mouse lymphoma cells (L5178YMDR), demonstrating to be a strong MDR reversal agent in both (14). Methoxyboetirane B (Figure 5), a derivative of the macrocyclic diterpene epoxyboetirane A (Figure 5), isolated from *Euphorbia boetica* Boiss., was evaluated for its anti-MDR potential in the same cell lines, being the one that, among other 22 derivates, demonstrated the most promising activity for the development of MDR-reversing agents (49).

A small library of jolkinol D (Figure 5) derivatives, a macrocyclic diterpene isolated from *Euphorbia piscatoria*, was synthesized. The derivatives were evaluated for their ability to reverse ABCB1-mediated MDR. The results showed that addition of electron-donating groups to the aromatic moieties improved the activity. Some derivates were evaluated for their collateral sensitivity effect against the human cancer cells EPG85−257 (gastric) and EPP85−181 (pancreatic), and the corresponding drug-selected cells EPG85-257RDB, EPG85-257RNOV, EPP85-181RDB, and EPP85-181RNOV. Some of the compounds were more cytotoxic against the resistant sublines. They were found to induce apoptosis through caspase-3 activation, with noticeable differences between parental and resistant cells (50). Other examples of the anti-MDR potential of macrocyclic diterpenes of the jatrophane and lathyrane-type isolated from *Euphorbia* species, are reported, being the key factor for their inhibition potential their hydrophobicity (51).

The lathyrane jatrofoliane B (Figure 5), isolated from *Jatropha gossypiifolia* Linn (Euphorbiaceae), has shown effects comparable to the 1st generation inhibitor verapamil, in regards to HepG2/ADR and HCT-15/5-FU cell lines, but with less toxicity (52). Nicaeenin G (Figure 5), a jatrophane isolated from *Euphorbia nicaeensis*, was tested as P-gp inhibitor in two human MDR-resistant cell lines: non-small cell lung carcinoma NCI-H460/R and colorectal

carcinoma DLD1-TxR. From all the compounds tested in this study, Nicaeenin G was the most potent inhibitor and showed a prolonged effect comparable do dexverapamil, a known 2nd-generation inhibitor (53).

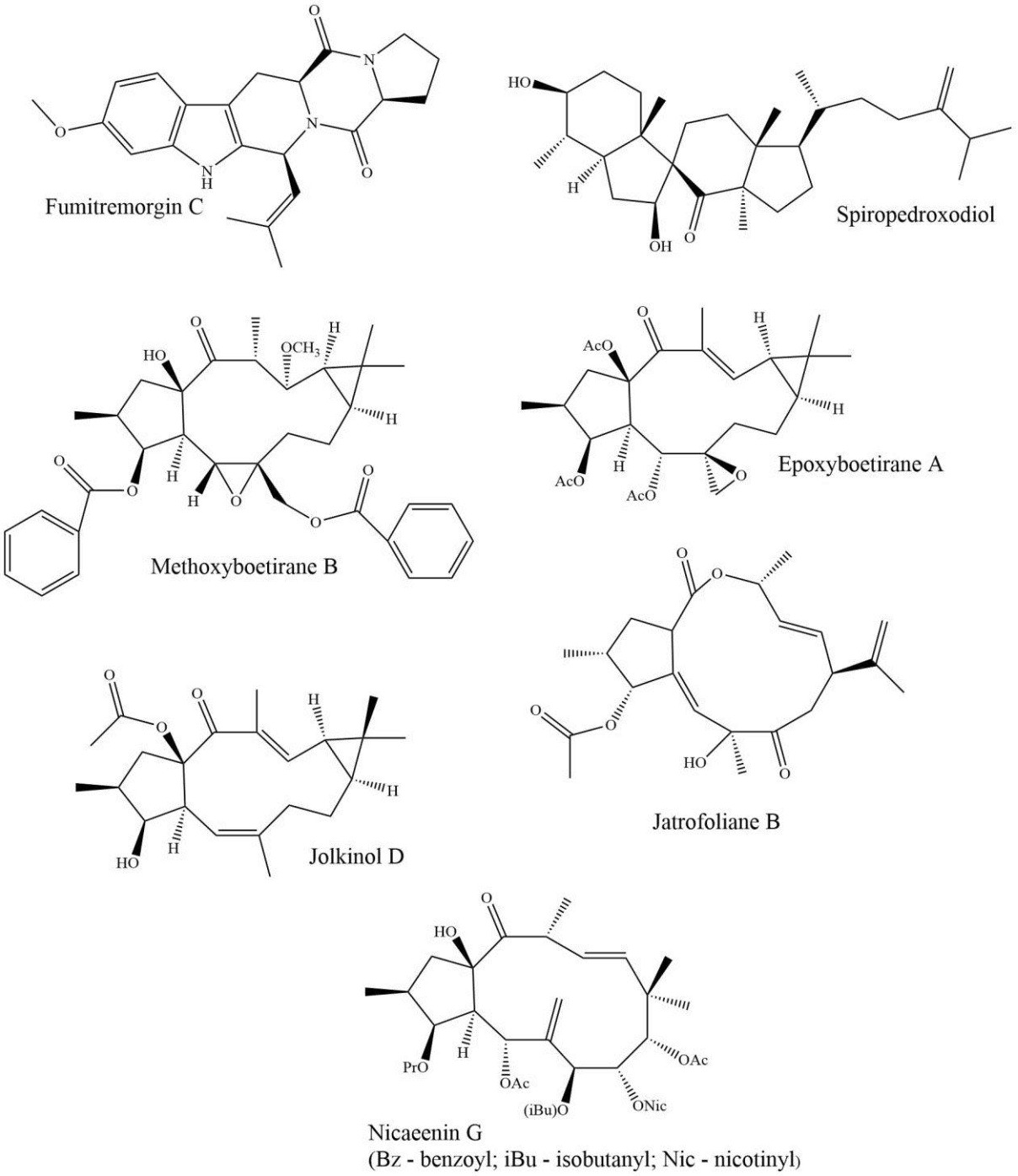

***Figure 5** - Structure of a few 4th generation modulators.*

Aim of this work

The aim of this project was to find out new bioactive compounds from *Euphorbia pubescens*. To achieve this goal, the work was divided in two parts. Firstly, the phytochemical study of three fractions of *E. pubescens* methanol extract was carried out, using chromatographic techniques. Then, the molecular manipulation of taraxerone, a pentacyclic triterpene isolated in large amounts, was also performed, taking advantage of the ketone function at C-3. Overall, fourteen compounds were obtained and characterized through spectroscopic techniques.

Results and Discussion

1.5 Phytochemical Study of *Euphorbia pubescens*

The phytochemical study of *E. pubescens* aerial parts led to the isolation of ten terpenic compounds, including five pentacyclic triterpenes (**1-3, 5** and **6**), one steroid (**4**), one jatrophane-type diterpene (**7**), and three *ent*-abietane diterpenic lactones (**8-10**). Moreover, one phenolic compound was also isolated (**11**).

This section presents the description and discussion of physical and spectroscopic data that allowed the structural identification of all the isolated compounds.

1.5.1 Taraxerone

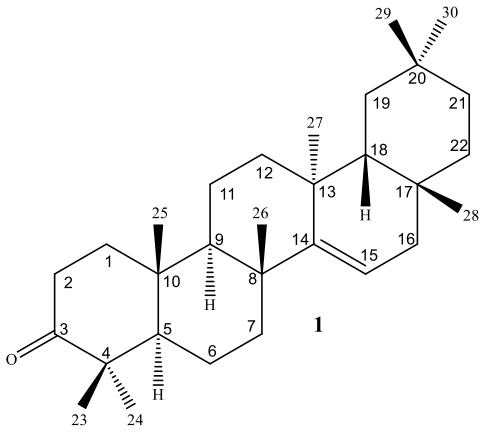

Compound **1** was isolated as white crystals, with a melting point of 141-143 °C and $[\alpha]_D^{25}$ +50.0.

The IR spectrum presented a characteristic absorption band, for the carbonyl group (1708 cm^{-1}). The ESI-MS spectrum showed a protonated molecular ion at *m/z* 425 $[M+H]^+$, that together with the analysis of the NMR data were indicative of the molecular formula $C_{30}H_{48}O$ (seven degrees of unsaturation), pointing out to the existence of a pentacyclic triterpenic scaffold.

The ^{1}H-NMR spectrum (Table 3) showed the presence of eight tertiary methyl groups displayed as singlets at δ_H 1.14, 1.08 (2 x CH_3) 1.07, 0.95, 0.91 (2x CH_3) and 0.83, and one olefinic proton displayed as a double doublet at δ_H 5.56 (*J* = 8.2 and 3.3 Hz).

The ^{13}C-NMR spectrum (Table 4) showed the presence of thirty signals that were discriminated by a DEPT experience as eight quaternary carbons (one olefinic at δ_C 157.77 and

one carbonyl at δ_C 217.70), four methines (one sp^2 at δ_C 117.35), ten methylenes and eight methyl groups.

From this information, and by comparison with the literature(39), compound **1** was identified as taraxerone.

Table 3 *- ^{1}H-NMR data of taraxerone (**1**), taraxerol (**2**) and taraxerol acetate (**3**) ($CDCl_3$,300 MHz, δ in ppm, J in Hz).*

Position	1	2	3
3		3.19 *dd* (*J* = 15.6, 5.4)	4.46 (*dd*, *J* = 9.8, 6.2)
15	5.56 dd (*J* = 8.2, 3.3)	5.53 *dd* (*J* = 8.2, 3.3)	5.53 (*dd*, *J* = 8.1, 3.2)
23	1.08 *s*	0.98 *s*	0.95 *s**
24	1.07 *s*	0.93 *s*	0.82 *s*
25	1.08 *s*	0.80 *s*	0.90 *s**
26	0.91 *s**	0.91 *s**	1.09 *s*
27	1.14 *s*	1.09 *s*	0.87 *s*
28	0.83 *s*	0.82 *s*	0.86 *s*
29	0.95 *s*	0.95 *s*	0.95 *s**
30	0.91 *s**	0.91 *s**	0.90 *s**
$COCH_3$			2.04 *s*

*Overlapped signals.

Table 4 *- ^{13}C-NMR data of taraxerone (**1**), taraxerol (**2**) and taraxerol acetate (**3**) ($CDCl_3$, 75 MHz, δ in ppm).*

Position	DEPT	1	2	3
1	CH_2	38.51	38.16	37.84*
2	CH_2	34.29	27.31	28.95
3	C (**1**) / CH (**2, 3**)	217.70	79.23	81.17
4	C	47.73	38.92	39.14
5	CH	55.94	55.69	55.80
6	CH_2	20.12	18.95	18.84
7	CH_2	35.26	35.28	35.27
8	C	39.03	39.14	38.05
9	CH	48.86	48.92	48.93
10	C	35.93	37.90	37.84*
11	CH_2	17.60	17.66	17.66
12	CH_2	37.90	35.94	35.93
13	C	37.85	37.87	37.55
14	C	157.77	158.25	158.14
15	CH	117.35	117.03	117.09
16	CH_2	36.83	36.84	36.82
17	C	37.70	37.73	37.71
18	CH	48.96	49.44	49.35
19	CH_2	40.80	41.49	41.38
20	C	28.95	28.95	29.98
21	CH_2	33.73	33.86	33.83
22	CH_2	33.24	33.26	33.25
23	CH_3	26.27	28.15	28.13
24	CH_3	21.50	15.58	15.64
25	CH_3	14.96	15.6	16.73
26	CH_3	30.01	30.08	31.06
27	CH_3	25.72	26.06	26.07
28	CH_3	30.07	29.98	30.07
29	CH_3	33.51	33.51	33.49
30	CH_3	21.63	21.47	23.61
$COCH_3$	C			171.12
$COCH_3$	CH_3			21.43

*Overlapped signals.

Taraxerone has shown to possess anti-tumoral (K562 leukemic cell line and A-549 lung cancer cells) (40,41) and anti-leishmanial [*Leishmania donovani* (strain AG 83)] (40) activity.

1.5.2 Taraxerol

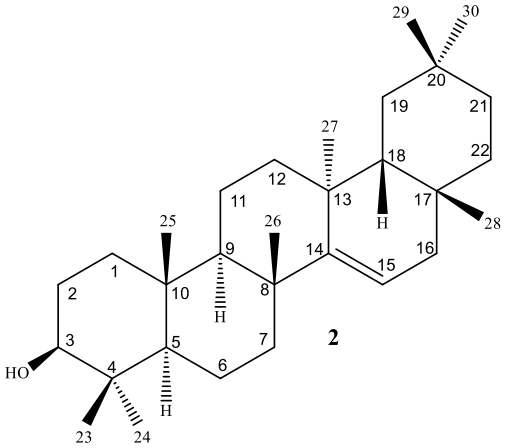

Compound **2** was isolated as an amorphous white powder and $[\alpha]_D^{25}$ +80.0.

The IR spectrum presented an absorption band at 3487 cm^{-1}, indicating the presence of a hydroxyl group, which was corroborated by the ESI-MS spectrum that revealed an ion at *m/z* 409 $[M+H-H_20]^+$.

A comparison of the NMR data of compound **2** with those of taraxerone (**1**) showed that the ^1H and ^{13}C chemical shifts are almost identical, except those for ring A (Tables 3 and 4). In fact, the major differences in the NMR spectra were the absence of the carbonyl signal at δ_C 217.70 and the appearance of an oxymethine signal at δ_H 3.19 (*dd*, *J* = 15.6 and 5.4 Hz) and δ_C 79.23.

The identity of compound **2** as taraxerol was confirmed by comparison of all spectroscopic data to those reported in the literature (42).

Taraxerol has shown to be able to reduce HeLa cells survival rate by suppressing the PI3K/Akt signaling pathway, thus promoting apoptosis (43). It has also shown inhibitory effects against sarcoma 180 cell line in mice, and is known to be beneficial against diabetes, Parkinson and Alzheimer's (44).

1.5.3 Taraxerol Acetate

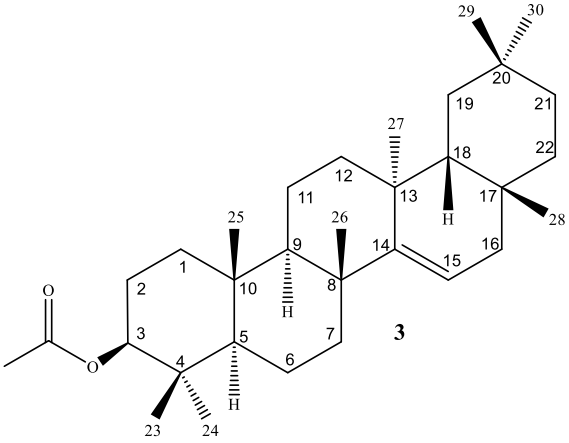

Compound **3** was isolated as an amorphous white powder and $[\alpha]_D^{25}$ +55.5.

Its IR spectrum displayed an absorption band for an ester group (1724 and 1252 cm^{-1}) and the ESI-MS spectrum showed an ion at *m/z* 409 $[M+H-C_2H_4O_2]^+$.

A comparison of the NMR data of compound **3** with those of taraxerol (**2**) showed that the ^1H and ^{13}C chemical shifts were almost identical, except those for ring A (Tables 3 and 4), with the major differences being the appearance of the acetyl group signals at (δ_H 2.04; δ_C 171.12 and 21.43) and the downfield shift of the oxymethine signal that appeared at δ_H 4.46 (*dd*, *J* = 9.8 and 6.2 Hz).

Due to similarities of the spectroscopic data with those of taraxerone (**1**) and taraxerol (**2**), and by comparing the obtained data with the literature(45), compound **3** was identified as taraxerol acetate.

Taraxerol acetate has demonstrated anti-cancer activity against U87 cells, mediated through apoptosis, autophagy, cell cycle arrest and inhibition of cell migration (46). It also showed anti-pyretic (47) and anti-inflammatory activities (48).

1.5.4 β-Sitosterol

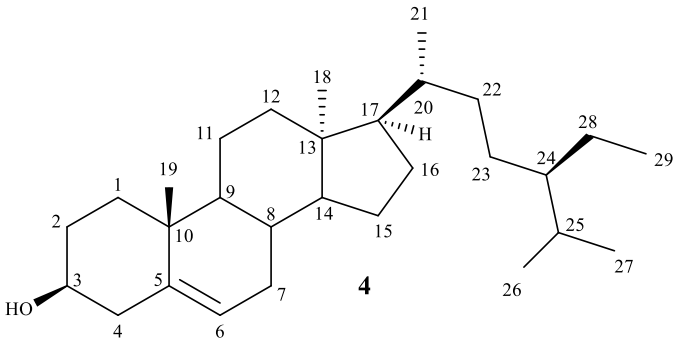

Compound **4** was isolated as white crystals, m.p. 130-131 °C and $[\alpha]_D^{25}$ -15.8.

In the IR spectrum a characteristic absorption band for hydroxyl group (3421 cm^{-1}) was observed. The ESI-MS spectrum showed an ion at *m/z* 397 $[M+H-H_2O]^+$.

The ^{1}H-NMR spectrum showed signals for six methyl groups, namely two tertiary (δ_H 0.68 and 1.01), three secondary displayed as doublets at δ_H 0.80 (*d*, *J* = 6.6 Hz), 0.83 (*d*, *J* = 6.6 Hz) and 0.92, and one primary at δ_H 0.86 (*t*, *J* = 7.2 Hz). Moreover, this spectrum also showed the presence of a multiplet at δ_H 3.51 and a doublet at δ_H 5.34, signals that were assigned to an oxymethine and olefinic protons, respectively (Table 5).

The analysis of the ^{13}C-NMR spectrum revealed twenty-nine signals, which were discriminated by a DEPT experiment as three quaternary carbons (one olefinic at δ_C 140.93), nine methines (one oxygenated at δ_C 71.77 and one olefinic at δ_C 121.67), eleven methylenes and six methyl carbons (Table 6). From this data it was clear that compound **4** was a Δ^5-3β-hydroxy sterol.

By comparison of all the spectroscopic data with those described in the literature(49), compound **4** was unambiguously identified as β-sitosterol.

***Table 5** - ^{1}H-NMR data of ß-sitosterol (**4**) ($CDCl_3$, 300 MHz, δ in ppm, J in Hz).*

Position	4
3	3.52 *m*
6	5.35 *d* (5.4)
18	0.68 *s*
19	1.01 *s*
21	0.92 *d* (6.5)
26	0.80 *d* (*J* = 6.6)
27	0.83 *d* (*J* = 6.5)
29	0.86 *t* (*J* = 7.2)

Table 6 *- ^{13}C-NMR data of ß-sitosterol (**4**) ($CDCl_3$, 75 MHz, δ in ppm).*

Position	DEPT	4	Position	DEPT	4
1	CH_2	37.42	**15**	CH_2	26.26
2	CH_2	31.85	**16**	CH_2	28.20
3	CH	71.77	**17**	CH	56.23
4	CH_2	42.27	**18**	CH_3	36.30
5	C	140.93	**19**	CH_3	18.99
6	CH	121.67	**20**	CH	34.12
7	CH_2	32.08	**21**	CH_3	26.06
8	CH	31.64	**22**	CH_2	46.02
9	CH	50.31	**23**	CH_2	23.24
10	C	36.67	**24**	CH	11.93
11	CH_2	21.04	**25**	CH	29.13
12	CH_2	39.79	**26**	CH_3	19.76
13	C	42.49	**27**	CH_3	19.35
14	CH	56.73	**28**	CH_2	18.73
			29	CH_3	11.81

β-sitosterol has shown to have anti-cancer activity against TPA-induced EBV-EA activation in Raji cells, as PI3K inhibitor (50); MCF-7 tumor cell lines and MDA-MB-231 human breast cancer cell line (51). It also displayed good analgesic and anti-inflammatory activities, working through central mechanism by opioid receptors (52).

1.5.5 Isomultiflorenol

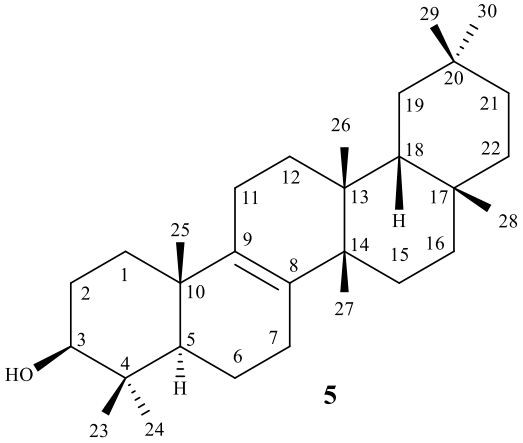

5

Compound **5** was isolated as an amorphous white powder and $[\alpha]_D^{25}$ +88.2.

The IR spectrum exhibited an absorption band at 3410 cm^{-1} that together with the ion at m/z 409 $[M+H-H2O]^+$ in the ESI-MS suggested the presence of a hydroxyl group.

The ^{1}H-NMR spectrum (Table 7) showed a double doublet signal corresponding to an axial oxymethine proton at δ_H 3.23 (*J* = 11.4 and 4.8 Hz) and signals for eight tertiary methyl groups (δ_H 1.07, 1.06, 1.00, 0.99, 0.97, 0.96 (2 x CH_3) and 0.80).

The ^{13}C-NMR spectrum presented thirty signals that were discriminated by a DEPT experiment as eight quaternary carbons (two olefinic at δ_C 133.67 and 135.24), three methines (one oxygenated at δ_C 79.18), eleven methylenes and eight methyl carbons (Table 8).

By comparison of all spectroscopic data with those reported in the literature(53), compound **5** was undoubtedly identified as isomultiflorenol.

Table 7 *- ^{1}H-NMR data of isomultiflorenol (**5**) and isomultiflorenyl acetate (**6**) ($CDCl_3$, 300 MHz, δ in ppm, J in Hz).*

Position	5	6	Position	5	6
3	3.23 *dd* (*J* = 11.4, 4.8)	4.48 *dd* (*J* = 11.3, 6.5)	**27**	0.97 *s*	1.05 *s*
23	0.80 *s*	0.87 *s*	**28**	1.07 *s*	1.07 *s*
24	0.96 *s**	0.88 *s*	**29**	0.99 *s*	0.95 *s*
25	0.96 *s**	0.97 *s**	**30**	1.00 *s*	0.97 *s**
26	1.06 *s*	0.97 *s**	**$COCH_3$**		2.05 *s*

*Overlapped signals

Table 8 *- ^{13}C-NMR data of compounds **5** and **6** ($CDCl_3$, 75 MHz, δ in ppm).*

Position	DEPT	5	6	Position	DEPT	5	6
1	CH_2	34.34	34.76	**28**	CH_3	31.65	31.63
2	CH_2	24.84	24.32	**29**	CH_3	34.66	34.45
3	CH	79.18	81.10	**30**	CH_3	33.14	33.07
4	C	38.96	37.84	**COCH$_3$**	C		171.25
5	CH	50.86	50.87	**COCH$_3$**	CH_3		21.49
6	CH_2	19.39	19.20				
7	CH_2	28.08	27.46				
8	C	135.24	135.23				
9	C	133.67	133.45				
10	C	37.77	37.56				
11	CH_2	20.96	20.94				
12	CH_2	30.84	30.74				
13	C	37.44	37.35				
14	C	41.14	41.11				
15	CH_2	27.65	26.30				
16	CH_2	36.85	36.83				
17	C	30.95	30.90				
18	CH	44.27	44.23				
19	CH_2	34.55	34.31				
20	C	28.48	28.45				
21	CH_2	35.20	43.11				
22	CH_2	36.96	36.81				
23	CH_3	28.20	16.83				
24	CH_3	15.76	28.11				
25	CH_3	19.97	20.00				
26	CH_3	19.12	19.04				
27	CH_3	26.41	24.74				

1.5.6 Isomultiflorenyl Acetate

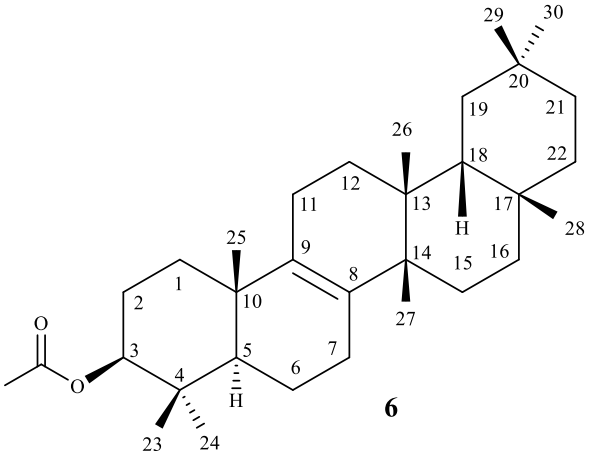

6

Compound **6** was isolated as an amorphous white powder and $[\alpha]_D^{25}$ +98.8.

The IR spectrum was similar to compound **5**, except for the absence of the hydroxyl absorption band and the presence of additional absorption bands for the ester carbonyl group at 1726 cm^{-1} and 1250 cm^{-1}.

A comparison of the NMR data of compound **6** with those of isomultiflorenol (**5**) showed that the ^{1}H and ^{13}C chemical shifts were almost identical, except those for ring A (Table 7 and 8). The major differences were the presence of an acetyl group at C-3 (δ_C 81.10), indicated by the downfield shift of oxymethine signal (δ_H 4.48 *dd* (*J* = 11.3 and 6.5 Hz) and by the existence of the acetyl signals at δ_H 2.05 (*s*) and δ_C 171.25 and 21.49. The presence of the acetyl group was also confirmed by the ESI-MS spectrum that showed an ion at m/z 409 $[M+H-C_2H_4O_2]^+$.

With all this information, and through comparison with isomultiflorenol and the data reported from literature(54), compound **6** was unambiguously identified as isomultiflorenyl acetate.

1.5.7 Euphopubescenol

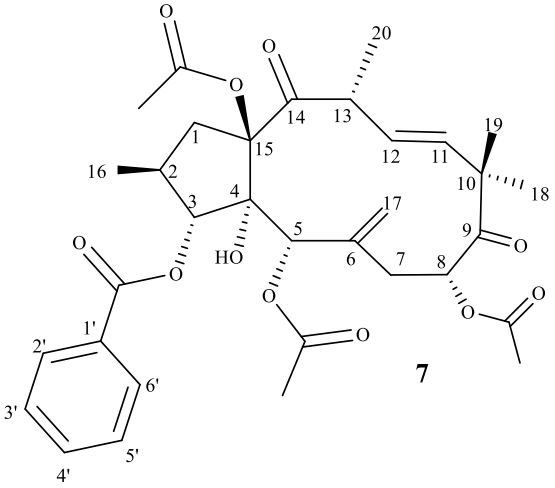

7

Compound **7** was isolated as an amorphous white powder and with a $[\alpha]_D^{25}$ +74.6.

The IR spectrum revealed a band at 3520 cm^{-1} for a hydroxyl group and bands at 1748 and 1715 cm^{-1} for carbonyl groups (carbonyl ester and ketone, respectively). A band at 1633 cm^{-1} supports the presence of at least double bond. The ESI-MS spectrum showed an ion at *m/z* 553 $[M+H-CH_3COOH]^+$.

The ^{1}H-NMR spectrum showed two signals for tertiary methyls at δ_H 1.46 and 1.22, two secondary methyls as doublet signals at δ_H 1.38 (*J* = 6.5 Hz) and 1.24 (*J* = 6.9 Hz), two doublet signals and one singlet for protons geminal to ester groups at δ_H 5.67 (*J* = 8.9 Hz), 5.61 (*J* =

10.5 Hz) and δ_H 4.86. Moreover, signals corresponding to one exocyclic double bond indicated by two singlets at δH 4.86 and 5.12 and a *trans*-disubstituted one (δ_H 5.89 *d*, *J* = 9.0 Hz, and 5.92 *dd*, *J* = 16.0, 9.0 Hz) were also observed. In addition, one benzoate group (δ_H 7.42, 7.57 and 7.97) and three acetyl groups (at δ_H 1.91, 2.08 and 2.16) were also identified. Also noteworthy is the presence of a signal at δ_H 3.46 without correlation in the HMQC spectrum, which suggested the presence of a tertiary hydroxyl group in the molecule (Table 9).

In the ^{13}C-NMR, thirty-one carbon signals were present, but as eleven of these signals belonged to the ester functions, the remaining twenty carbon signals were assigned to the main scaffold and were, through a DEPT experience, sorted as six quaternary carbons (two carbonyl groups at δ_C 208.20 and 204.61, two oxygenated carbons at δ_C 82.94 and 94.62, and one sp^2 carbon at δ_C 140.17), seven methines (two sp^2 at δ_C 136.91 and 132.84 , and three oxygenated at δ_C 77.89, 73.28 and 72.41), three methylenes (one sp^2 at δ_C 116.89) and four methyl groups (Table 10).

On the basis of all these data, a jatrophane-type skeleton was proposed for compound **7**. The unambiguous assignment of all proton and carbon resonances was possible through the combined analysis of 2D-NMR spectra, namely COSY, HMQC and HMBC (Figure 6).
In particular, ^{1}H-^{1}H-COSY and HMQC spectra defined four structural fragments (A-D) with correlated protons (Figure 6), which are separated by quaternary carbons. The linkage of fragments A and D was possible through the $^2J_{C\text{-}H}$ and $^3J_{C\text{-}H}$ correlations displayed in the HMBC spectrum, namely, those between C-15 and H-1 and those between C-14 and H-1 and H-20. Moreover, heteronuclear $^2J_{C\text{-}H}$ and $^3J_{C\text{-}H}$ correlations allowed the assignment of the ketone function at C-9, which was connected with the fragment D due to the observed cross peaks between C-9 with H-18 and H-19, and C-10 with H-11 and H-12.

Analysis of the HMBC spectrum also allowed the connection between fragments B and C, sustained by the correlations found between C-6 with H-7 and H-8 together with those between C-8 and H-17α and H-17β. The linkage of fragments B and A was possible due to the correlations found between C-6 and H-5, and those found between C-15 and C-17 with H-5, together with the information found in the literature. Analysis of HMBC spectrum additionally permitted to establish the position of the benzoyl group at C-3 and acetate groups at C-5 and C-8. All the spectroscopic data were in agreement to those described in the literature for euphopubescenol. (55)

Table 9 *- ^{1}H-NMR data of euphopubescenol (**7**) ($CDCl_3$, 300 MHz, δ in ppm, J in Hz).*

Position	7	Position	7
1	2.43 *m**	**17**	4.85 *s* (H-α) / 5.12 *s* (H-β)
2	2.91 *tdd* (*J* = 10.4, 7.0, 3.5)	**19**	1.46 *s*
3	5.61 *d* (*J* = 10.5)	**20**	1.38 *d* (*J* = 6.5)
5	4.86 *s*	**Bz (2',6')**	7.97 *dd* (*J* = 8.0; 1.5)
7	1.71 *dd* (*J* = 14.9, 9.2, H-α) / 2.00 s (H-β)	**Bz (3',5')**	7.42 *t* (*J* = 7.8)
8	5.67 *d* (*J* = 8.9)	**Bz (4')**	7.57 *tt* (*J* = 7.5, 1.5)
11	5.89 *d* (*J* = 9.0)	**5-O($COCH_3$)**	2.08 *s*
12	5.92 *dd* (*J* = 16.0, 9.0)	**8-O($COCH_3$)**	1.91 *s*
13	3.85 *m*	**15-O($COCH_3$)**	2.16 *s*
16	1.24 *d* (*J* = 6.9)	**18**	1.22 *s*

* This value corresponds to either protons 1α and 1β.

Table 10 *- ^{13}C-NMR data of euphopubescenol (**7**) ($CDCl_3$, 75 MHz, δ in ppm).*

Position	DEPT	7	Position	DEPT	7
1	CH_2	38.82	**17**	CH_2	116.89
2	CH	36.90	**18**	CH_3	24.57
3	CH	77.89	**19**	CH_3	24.57
4	C	82.94	**20**	CH_3	20.16
5	CH	73.28	**3-OBz**	C	166.60
6	C	140.17	**Bz (1')**	C	129.09
7	CH_2	35.97	**Bz (2',6')**	CH	130.19
8	CH	72.41	**Bz (3',5')**	CH	128.53
9	C	208.20	**Bz (4')**	CH	133.70
10	C	50.66	**5-O($COCH_3$)**	C	168.42
11	CH	136.91		CH_3	20.71
12	CH	132.84	**8-O($COCH_3$)**	C	169.87
13	CH	46.91		CH_3	20.42
14	C	204.61	**15-O($COCH_3$)**	C	168.86
15	C	94.62		CH_3	21.14
16	CH_3	17.79			

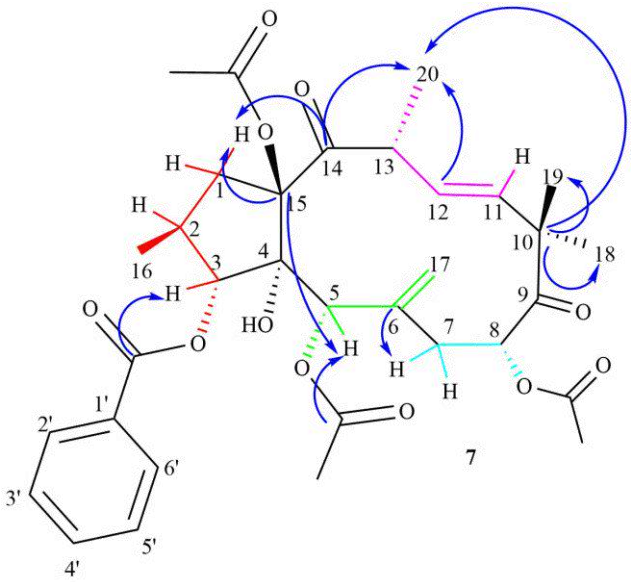

Figure 6 *- Euphopubescenol, with the colored lines indicating the different ^{1}H-spin systems, assigned through HMQC and ^{1}H-^{1}H COSY, and respective correlations displayed in the HMBC spectrum (indicated by arrows).*

Euphopubescenol (**7**) has demonstrated activity as inhibitor of multidrug transporters in *Saccharomyces cerevisiae* cells overexpressing the CaCdr1p ABC-transporter (AD-CDR1) (56), and also showed anti-tumoral activity as it inhibited the growth of MCF-7 and NCI-H460 cancer cell lines (55).

1.5.8 Helioscopinolide A

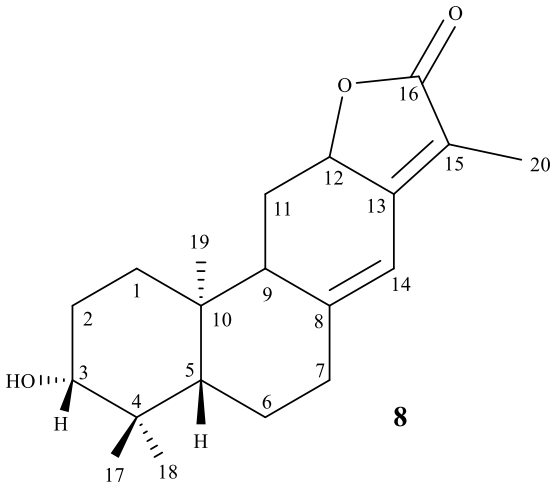

Compound **8** was isolated as white crystals, with m.p. of 204-206 °C and $[\alpha]_D^{25}$ +587.4.

The IR spectrum indicated the presence of a hydroxyl function (3478 cm^{-1}), and an unsaturated lactone (1734 cm^{-1}). The ESI-MS spectrum showed a protonated molecular ion at m/z 317 $[M+H]^+$, that together with the analysis of the NMR data were indicative of the molecular formula $C_{20}H_{28}O_3$ (seven degrees of unsaturation).

The ^{1}H-NMR spectrum (Table 11) showed three singlets for tertiary methyl groups at δ_H 0.81, 0.92, 1.02, and one vinylic methyl group at δ_H 1.81 (*d*, *J* = 1.7 Hz). Signals corresponding to two oxymethine protons at δ_H 3.27 (*dd*, *J* = 11.6 and 4.4 Hz) and 4.85 (*ddd*, *J* = 13.6, 6.2 and 1.8), and one olefinic proton at δ_H 6.27 (s), were also observed.

The ^{13}C-NMR spectrum (Table 12) exhibited twenty carbons resonances, that were discriminated by a DEPT experiment as four methyl groups (one vinylic at δ_C 8.37), five methylenes, five methines (one olefinic at δ_C 114.31 and two oxygenated at δ_C 76.0 and 78.66), and six quaternary carbons (three sp^2 carbons at δ_C 116.61, 151.58 and 156.17 and one carbonyl group at δ_C 175.39).

On the basis of all these data and by the comparison with the literature (57), compound (**8**) was identified as the *ent*-abietane diterpenic lactone helioscopinolide A.

Table 11 *- ^{1}H-NMR data of helioscopinolide A (**8**), helioscopinolide B (**9**) and helioscopinolide E (**10**) ($CDCl_3$, 300 MHz, δ in ppm, J in Hz).*

Position	8	9	10
1	1.94 *dt* (*J* = 13.1, 3.6)	1.60-1.70 *m**	2.22 *m**
2	1.64 *m*	1.60-1.70 *m**	2.56 *m*
3	3.27 *dd* (*J* = 11.6, 4.4)	3.46 *t* (*J* = 2.7, 2.7)	
5	1.14 *dd* (*J* = 12.5, 2.5)	1.64 *m*	1.59 *m***
6		1.41 *m*	1.59 *m***
7		2.47 *dd* (*J* = 4.2, 2.3)	2.22 *m**
9	2.18 *dd* (*J* = 15.1, 9.0)	2.29 *d* (*J* = 8.7)	
11	2.53 *m*	2.56 *m*	1.59 *m***
12	4.85 *ddd* (*J* = 13.6, 6.2, 1.8)	4.86 *ddd* (*J* = 13.3, 6.1, 1.2)	4.87 *ddd* (*J* = 13.4, 6.1, 1.8)
14	6.27 *s*	6.25 *s*	6.33 *s*
17	1.02 *s*	0.98 *s*	1.13 *s*
18	0.81 *s*	0.86 *s*	1.05 *s*
19	0.92 *s*	0.93 *s*	1.08 *s*
20	1.81 *d* (*J* = 1.7)	1.81 *d* (*J* = 1.3)	1.84 *d* (*J* = 1.6)

*/** Overlapped signals

Table 12 *- ^{13}C-NMR data of helioscopinolide A (**8**), helioscopinolide B (**9**) and helioscopinolide E (**10**) ($CDCl_3$, 75 MHz, δ in ppm).*

Position	DEPT	8	9	10
1	CH_2	37.53	32.19	37.53
2	CH_2	27.70	25.81	34.53
3	CH (**8,9**) / C (**10**)	78.66	75.62	215.63
4	C	39.21	37.85	47.67
5	CH	54.48	48.41	45.90
6	CH_2	23.56	23.49	24.74
7	CH_2	37.04	37.14	36.73
8	C	151.58	152.23	150.30
9	CH	51.67	51.64	50.80
10	C	41.34	41.39	41.06
11	CH_2	27.66	27.56	27.94
12	CH	76.00	76.12	75.75
13	C	156.17	156.30	155.65
14	CH	114.31	114.12	114.87
15	C	116.61	116.37	117.87
16	C	175.39	175.45	175.17
17	CH_3	28.79	28.83	26.66
18	CH_3	15.71	22.33	21.93
19	CH_3	16.82	16.81	16.38
20	CH_3	8.37	8.33	8.45

Helioscopinolide A has shown activity against *Staphylococcus aureus* (58), and as an inhibitor of ROS and proinflammatory cytokines in LPS-stimulated BV2 microglial cells by suppressing the expression of COX-2 and iNOS and inhibiting the enzyme activity (59), showing to be promising as therapeutic agent in treatment of neurodegenerative and neuroinflammatory diseases.

1.5.9 Helioscopinolide B

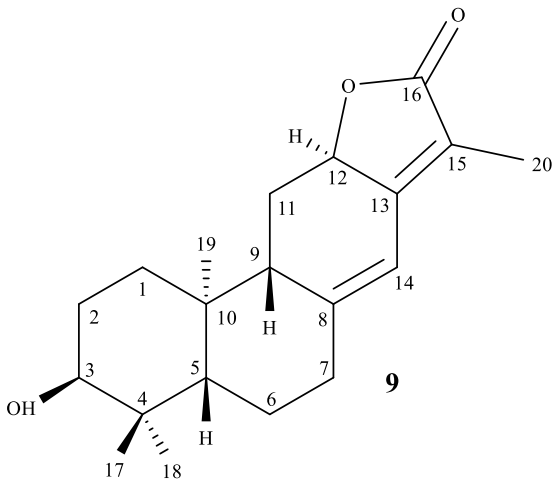

9

Compound **9** was isolated as a colorless oil and $[\alpha]_D^{25}$ +417.6.

The IR spectrum displayed absorption bands for hydroxyl 3467 cm^{-1} and for a lactone carbonyl group at 1730 cm^{-1}. The ESI-MS spectrum showed a protonated molecular ion at *m/z* 317 $[M+H]^+$, that together with the analysis of the NMR data were indicative of the molecular formula $C_{20}H_{28}O_3$ (seven degrees of unsaturation), pointing to the same structure as helioscopinolide A (**8**).

The NMR data for both compounds are very similar (Tables 11 and 12), with the exception of the signal of H-3. In compound **8** this signal appeared as a double doublet at δ_H 3.26 (*J* = 11.6 and 4.4 Hz). On the other hand, in compound **9**, H-3 signal is a triplet located downfield at δ_H 3.46 (*J* = 2.7, 2.7 Hz). This difference could be justified by the different configuration at C-3.

Through comparison with the literature (60), and by analysis of the spectra obtained, compound **9** was identified as helioscopinolide B.

Helioscopinolide B, like helioscopinolide A, has shown activity against *Staphylococcus aureus* (58), and antineoplastic and MDR modulatory activities against gastric (EPG85-257), pancreatic (EPP85-181) and colon (HT-29) carcinomas and their resistant phenotypes (EPG85-257/RDB), being particularly effective against the drug-resistance sublines (61).

1.5.10 Helioscopinolide E

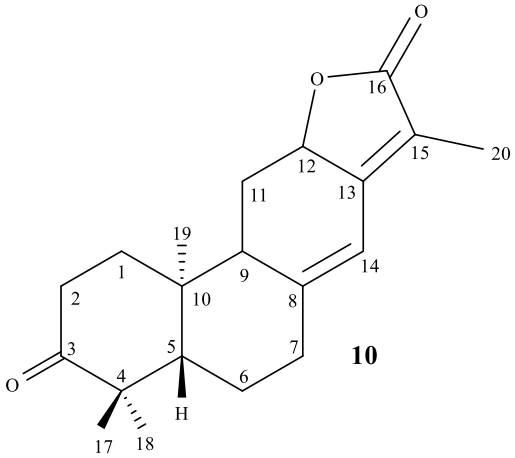

10

Compound **10** was isolated as a colorless oil and with a $[\alpha]_D^{25}$ +395.9.

The IR spectrum displayed strong absorption bands for carbonyl groups at 1706 cm^{-1} and 1751 cm^{-1}, and the ESI-MS spectrum showed a protonated molecular ion at *m/z* 317 $[M+H]^+$, that together with the analysis of the NMR data were indicative of the molecular

formula $C_{20}H_{26}O_3$ (eight degrees of unsaturation), suggesting a similar structure as helioscopinolide A (**8**) and B (**9**). Comparing the NMR spectra (Tables 11 and 12) of compound **10** with those of helioscopinolide B (**9**), the most important difference was the absence of the C-3 oxymethine signal (δ_H 3.46 and δ_C 75.62) that was replaced by ketone carbonyl group (δ_C 215.63).

Through analysis of the spectra, and comparison with helioscopinolide A, B and the literature (62), it was determined that compound **10** is helioscopinolide E.

Helioscopinolide E, like helioscopinolide B, has also shown promising antineoplastic and MDR modulatory activity against gastric (EPG85-257), pancreatic (EPP85-181) and colon (HT-29) carcinomas and their resistant phenotypes (EPG85-257/RDB) (61).

1.5.11 Coniferaldehyde

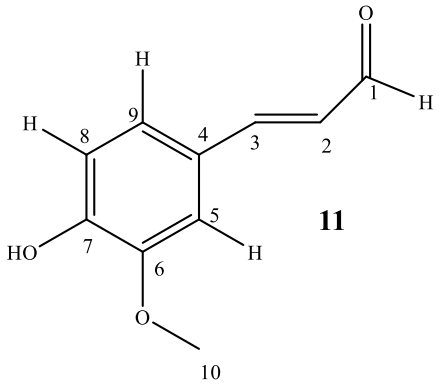

11

Compound **11** was isolated as an amorphous light-brown powder.

The IR spectrum showed an absorption band at 1691 cm^{-1} that is characteristic of unsaturated carbonyl groups. Bands at 3357 cm^{-1} and 1618 cm^{-1} suggested the presence of a hydroxyl group and an alkene, respectively. The protonated molecular ion at *m/z* 179 $[M+H]^+$ showed to be compatible with the molecular formula $C_{10}H_{10}O_3$ (six degrees of unsaturation), suggesting the presence of an aromatic ring and two double bonds.

The ^{1}H-NMR spectrum presented a methyl singlet at δ_H 3.94, and a signal belonging to the proton of an aldehyde function at δ_H 9.65 (*d*, *J* = 7.7 Hz). Also shown were the signals for protons of the benzene ring at δ_H 6.96 (*d*, *J* = 8.1 Hz), 7.07 (*d*, *J* = 1.9 Hz) and 7.12 (*dd*, *J* = 8.3, 2.0 Hz), and two signals for olefinic protons at δ_H 6.59 (*dd*, *J* = 15.8, 7.7 Hz) and 7.42 (*d*, *J* = 15.7 Hz) (Table 13).

The ^{13}C-NMR showed ten signals that were differentiated through DEPT, into three quaternary carbons (δ_C 126.80, 147.12 and 149.12), six methynes (the signal at δ_C 193.77 belonging to a carbon of an aldehyde group) and one methyl carbon (δ_C 56.15) (Table 14).

Taking into account the NMR data and comparison with the literature (63), compound **11** was identified as coniferaldehyde. All proton and carbon signals were unambiguous assigned by two-dimensional NMR experiments (Figure 7).

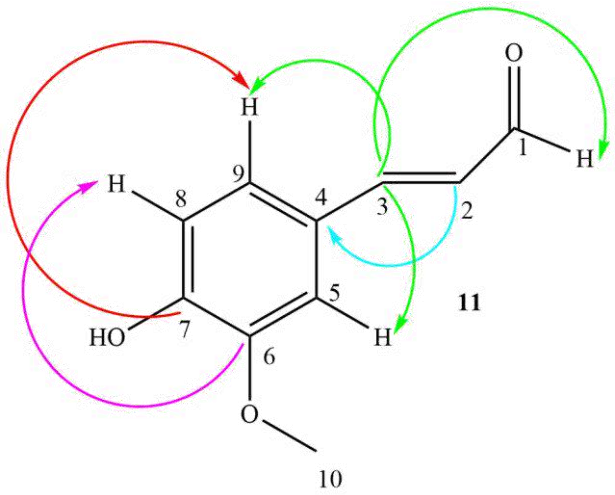

Figure 7 *- ^{3}JC-H correlations displayed in the HMBC spectrum of compound 11.*

Table 13- *^{1}H-NMR data of coniferaldehyde (**11**) ($CDCl_3$, 300 MHz, δ in ppm, J in Hz).*

Position	11
1	9.65 *d* (*J* = 7.7)
2	6.59 *dd* (*J* = 15.8, 7.7)
3	7.42 *d* (*J* = 15.7)
5	7.07 *d* (*J* = 1.9)
8	6.96 *d* (*J* = 8.1)
9	7.12 *dd* (*J* = 8.3, 2.0)
10	3.94 *s*

Table 14 *- ^{13}C-NMR data of coniferaldehyde (**11**) ($CDCl_3$, 300 MHz, δ in ppm).*

Position	DEPT	11
1	CH	193.77
2	CH	126.57
3	CH	153.24
4	C	126.80
5	CH	109.64
6	C	147.12
7	C	149.12
8	CH	115.10
9	CH	124.20
10	OCH_3	56.15

Coniferaldehyde has demonstrated to possess anti-microbial activity against zoospores, chlamydospores and mycelia of *Phytophthora ramorum* (64); anti-inflammatory activity as an effective inducer of HO-1 (an intrinsic cell-protective enzyme) and exerting anti-inflammatory properties in response to LPS (endotoxin components of gram-negative bacterial cell walls)(65). It also showed anti-oxidant and anti-radical activities (66).

It also demonstrated promising results as promotor of neuronal differentiation, as it facilitated neurite growth by ERK activation in Neuro2a cells with neurite growth blocked by an ERK inhibitor (66).

1.6 Derivatization of taraxerone (**1**)

Taraxerone (1) was isolated in higher quantity. Therefore, taking advantage of the ketone group, reactions with hydrazine, phenylhydrazine and 2,4-dinitrophenylhydrazine were successfully performed, yielding imines **1.1-1.3** (Scheme 4). The structures of the taraxerone hydrazones (**1.1-1.3**) were established through NMR experiments and by comparison of their spectroscopic data with those of taraxerone.

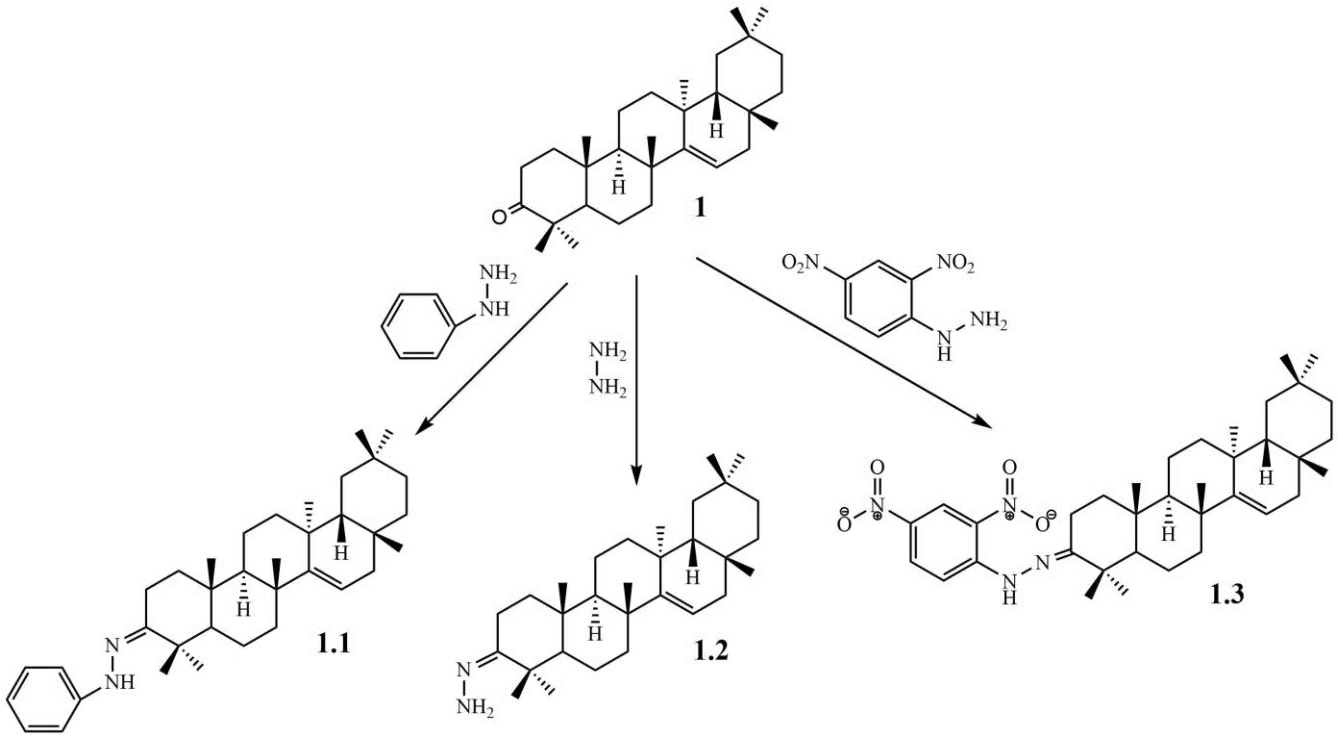

Scheme 4 *- Preparation of taraxerone derivatives (1.1 – 1.3). Conditions: hydrazines (5 eq), MeOH:CH2Cl2 (3:2), 200 µL of acetic acid 10%. This reaction occurred overnight under reflux.*

1.6.1 Structural identification of taraxerone derivatives

Compound **1.1** was obtained as a yellow amorphous solid with $[\alpha]_D^{25}$ +225.9. The ESI-MS spectrum showed a protonated molecular ion at *m/z* 513 $[M+H]^+$, which together with the analysis of the NMR data were indicative of the molecular formula $C_{36}H_{54}N_2$ (eleven degrees of unsaturation).

Compound **1.2** was obtained as a white amorphous solid with $[\alpha]_D^{25}$ +19.1. The ESI-MS spectrum revealed a protonated molecular ion at m/z 439 $[M+H]^+$, substantiating the molecular formula $C_{30}H_{50}N_2$ (six degrees of unsaturation).

Compound **1.3** was obtained as an orange amorphous solid with $[\alpha]_D^{25}$ +13.3, and the ESI-MS spectrum showed a protonated molecular ion at *m/z* 605 $[M+H]^+$, which together with the analysis of the NMR data were indicative of the molecular formula $C_{36}H_{52}N_4O_4$ (twelve degrees of unsaturation).

Through analysis of the IR spectrum, the presence of a secondary amine was suggested by a weak absorption band at 3300-3700 cm^{-1}. The disappearance of the band characteristic of carbonyl groups was noticeable. The presence of an aromatic ring was also shown through bands at 684/743 cm^{-1} in compounds **1.1** and **1.3.**

Besides the signals due to the different hydrazone moieties (**1.1** and **1.3**), the analysis of ^{1}H-NMR and ^{13}C-NMR spectra showed, as expected, very similar data regarding the triterpenic core (Tables 15 and 16). In fact, concerning the ^{13}C-NMR spectra, the most remarkable difference was the absence of the carbonyl signal of taraxerone at δ_C 217.70 that was replaced by a carbon signal at higher field (δ_C 148.31 for **1.1**, δ_C 151.11 for **1.2** and δ_C 167.31 for **1.3**), which corroborated the substitution of the carbonyl moiety by the corresponding imine.

Table 15 *- ^{1}H-NMR data of taraxerone derivatives **1.1**, **1.2** and **1.3** ($CDCl_3$, 300 MHz, δ in ppm, J in Hz).*

Position	1.1	1.2	1.3
15	5.54 *dd* (*J* = 8.1, 3.2)	5.55 *dd* (*J* = 8.3, 3.4)	5.56 *dd* (*J* = 8.2, 3.2)
24	1.09 *m*	1.04 *s*	1.07 *s*
25	1.07 *s*	1.11 *s*	1.18 *s*
26	0.95 *s*	0.91 *s*	0.90 *s*
27	1.14 *s*	1.21 *s*	1.15 *s*
28	0.84 *s*	0.83 *s*	0.83 *s*
29	0.96 *s*	0.95 *s*	0.95 *s*
30	0.92 *s*	0.89 *s*	0.92 *s*
2'	7.49 *dd* (*J* = 5.1, 2.0)		7.95 *d* (*J* = 9.6)
3'	7.49 *dd* (*J* = 5.1, 2.0)		8.29 *dd* (*J* = 9.6, 2.6)
4'	7.72 *m*		
5'	7.49 *dd*, (*J* = 5.1, 2.0)		9.12 *d* (*J* = 2.5)
6'	7.49 *dd* (*J* = 5.1, 2.0)		

Table 16 *- ^{13}C-NMR data of taraxerone derivatives **1.1, 1.2** and **1.3** ($CDCl_3$, 75 MHz, δ in ppm).*

Position	DEPT	1.1	1.2	1.3
1	CH_2	38.27	38.25	38.00
2	CH_2	33.93	27.80	28.54
3	C	151.11	148.31	167.31
4	C	42.50	41.80	42.49
5	CH	51.74	56.35	56.12
6	CH_2	18.78	20.00	20,17
7	CH_2	34.00	35.27	35.26
8	C	39.23	39.12	39.06
9	CH	48.86	48.95	48.83
10	C	35.30	35.93	35.94
11	CH_2	17.61	17.60	17,63
12	CH_2	37.88	38.08	37.85
13	C	37.71	37.86	37.68
14	C	158.15	158.08	157.77
15	CH	117.02	117.13	117.36
16	CH_2	35.95	36.83	36.83
17	C	36.86	37.70	37.56
18	CH	48.95	49.07	48.95
19	CH_2	41.25	41.11	40.91
20	C	26.22	28.95	28.94
21	CH_2	33.28	25.84	33.71
22	CH_2	30.10	33.25	33.23
23	CH_3	23.16	23.67	25.78
24	CH_3	21.43	21.47	20.65

Table 16 *- 13C-NMR data of taraxerone derivatives 1.1, 1.2 and 1.3 (CDCl3, 75 MHz, δ in ppm). (Cont.)*

25	CH_3	15.70	15.06	14.79
26	CH_3	28.97	30.01	30.01
27	CH_3	22.42	17.91	24.25
28	CH_3	30.01	30.08	30.07
29	CH_3	33.51	33.51	33.50
30	CH_3	21.49	23.43	21.49
$\underline{CO}CH_3$ (1) / 1'	C	131.32		137.65
$CO\underline{CH_3}$ (1)/ 2'	CH_3 (**1**)/ CH (**1.1**, **1.3**)	107.29		123.75
3'	CH	129.31		129.11
4'	CH (**1.1**) / C (**1.3**)	122.76		145.77
5'	CH	129.31		116.64
6'	CH (**1.1**) / C (**1.3**)	107.29		130.10

Several other reactions were attempted using different reagents (2-furoic hydrazide, 2-thiphenecarboxylic acid hydrazide, (4-aminobenzoyl) hydrazide, 4-chlorobenzhydrazide, 4-(trifluoromethyl) benzhydrazide and 9-indole-3-acetic hydrazide). However, due to the low yield obtained, it was not possible to perform reliable spectra in order to characterize the compounds, though perhaps in a larger scale better results could be obtained.

Conclusion

The purpose of this study was to find out bioactive terpenes through isolation and molecular derivatization of compounds isolated in large amounts. After the phytochemical study of three fractions of *Euphorbia pubescens* methanol extract, eleven compounds were isolated through the use of chromatographic procedures, such as column and preparative thin layer chromatography.

From the non-polar fractions A and B, five pentacyclic triterpenes were isolated, namely, taraxerone (**1**), taraxerol (**2**), taraxerol acetate (**3**), isomultiflorenol (**5**) and isomultiflorenol acetate (**6**). Moreover, β-sitosterol (**4**) was also isolated from these fractions. A macrocyclic diterpene polyester, euphopubescenol (**7**), three diterpenic lactones, helioscopinolide A, B and E (**8, 9** and **10**), and a phenylpropanoid derivative, coniferaldehyde (**11**) were isolated from the more polar fraction J.

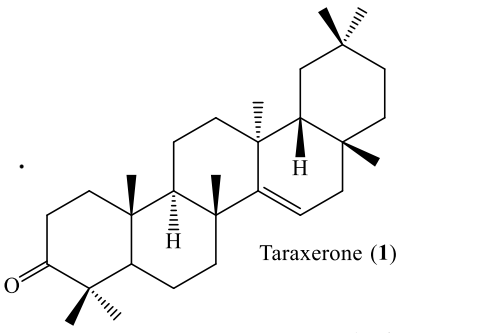

Taraxerone (**1**)

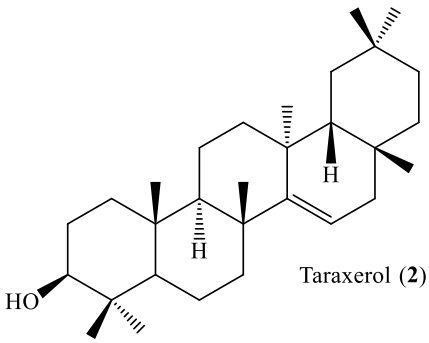

Taraxerol (**2**)

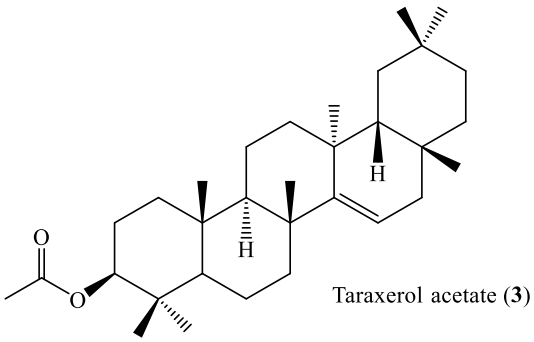

Taraxerol acetate (**3**)

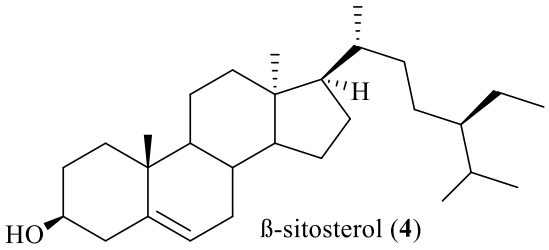

ß-sitosterol (**4**)

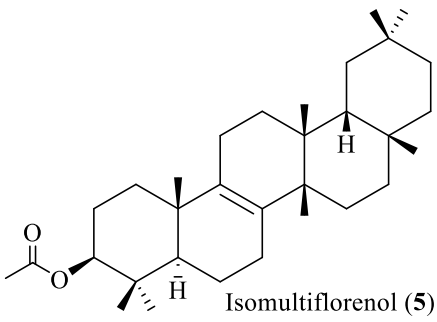

Isomultiflorenol (**5**)

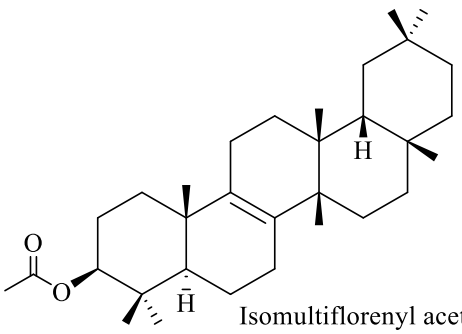

Isomultiflorenyl acetate (**6**)

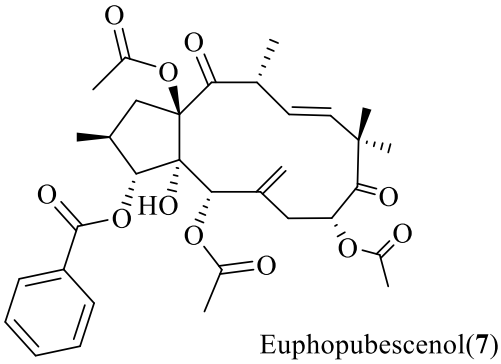

Euphopubescenol(**7**)

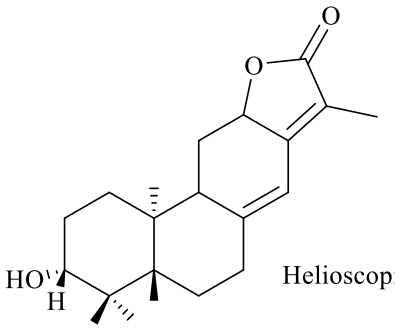

Helioscopinolide A (**8**)

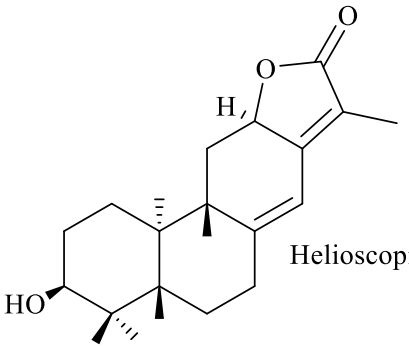

Helioscopinolide B (**9**)

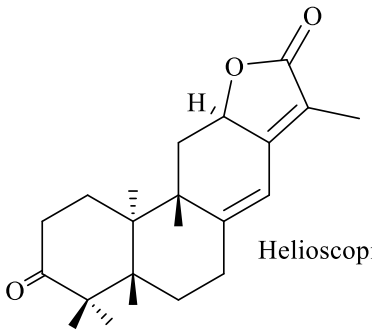

Helioscopinolide E (**10**)

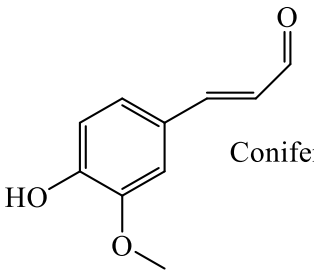

Coniferaldehyde (**11**)

The chemical structures of all compounds were ascertained through spectroscopic methods, including IR, MS, ^{1}H and ^{13}C NMR and 2D NMR (COSY, HMQC and HMBC experiments).

Taraxerone (**1)** was isolated in major amounts. Therefore, taking advantage of its carbonyl function, three hydrazine derivatives (**1.1** – **1.3**) were prepared through condensation with hydrazine, phenylhydrazine and 2,4-dinitrophenylhydrazine.

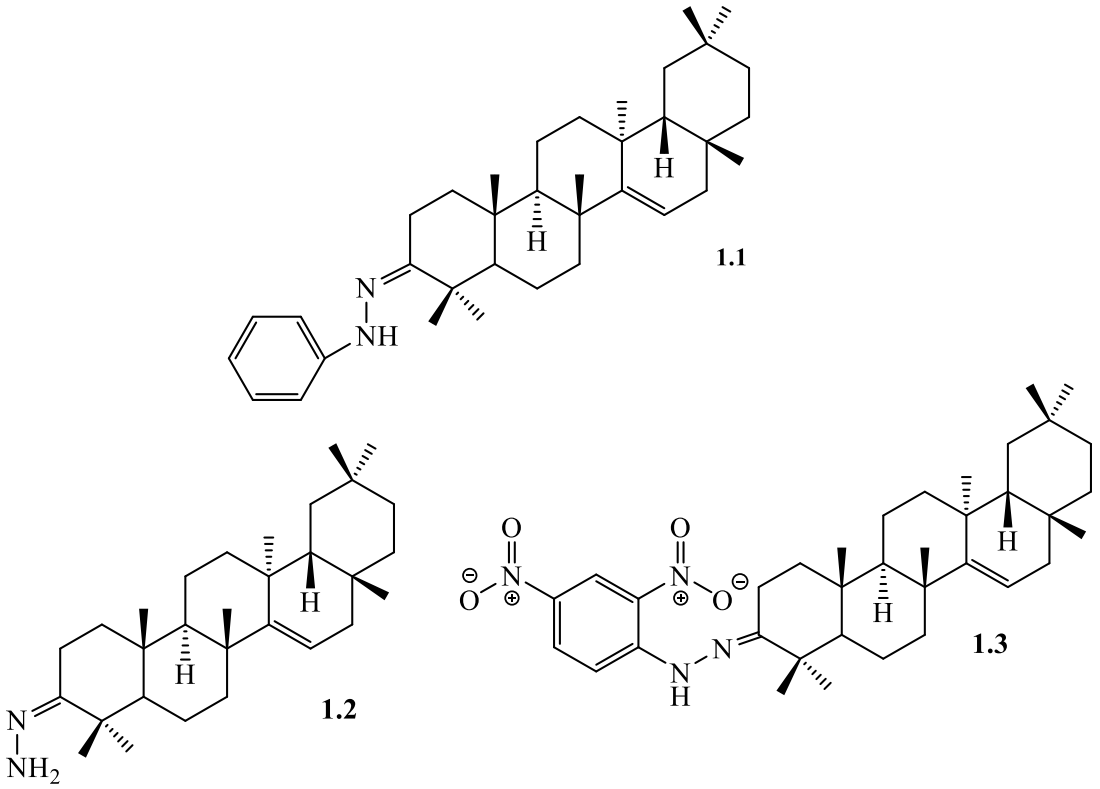

Euphorbia species have been used worldwide in traditional medicine in the treatment of ulcers, warts, skin affections and asthma. Therefore, in the last decades have been seen as an important source of bioactive compounds. Some of the compounds isolated in this work have shown promising results as anti-tumoral agents, including some that have demonstrated effectiveness as MDR modulators, as reported by other authors.

This work stands as a contribution for the phytochemical study of *Euphorbia pubescens*, corroborating the importance of natural products in the search of new drugs Continuing research of this species should follow, as just some parts were studied, and more compounds could be isolated and derivatized, leading to promising bioactive compounds.

The isolated compounds and derivatives will be further tested as P-gp modulators on multidrug resistant cancer cells overexpressing this transporter.

Experimental Section

1.7 General Procedures

All solvents were dried according to published methods and distilled prior to use. All the other reagents were obtained from commercial suppliers and were used without further purification.

Analytical thin layer chromatography (TLC) was performed on precoated silica-gel F254 plates (Merck 5554), visualized under UV light (254 and 366 nm) followed by spraying with H_2SO_4/MeOH (1:1) and finally heating the plate. Preparative TLC was carried out on 20 x 20 cm silica plates (Merck 5774). Column chromatography (CC) was performed over SiO_2 (Merck 9385) and over reverse-phase C18 silica (YMC-GEL ODS-A 12nm S-50µm AA12S50). CombiFlash® Rf 200 (Teledyne Isco) with SiO_2 or reverse-phase C18 prepacked columns were also used.

The NMR spectra were collected on a Bruker Fourier 300 spectrometer (^{1}H 300 MHz, ^{13}C 75 MHz) using $CDCl_3$ as solvent. ^{1}H and ^{13}C chemical shifts are expressed in δ (ppm) and the proton coupling constants (*J*) in hertz (Hz).

Melting points were determined on a Köpffler apparatus. Specific optical rotations were measured using a Jasco P-2000 digital polarimeter with a 1 dm long quartz cell and the samples were prepared in CHCl3.

Infrared (IR) spectra were collected on an Affinity-1 (Shimadzu) FTIR spectrophotometer in KBr pellets with only the most relevant absorption bands being reported.

Low resolution mass spectrometry (ESI-MS) was performed on a triple quadrupole (QT) mass spectrometer (Micromass Quattro Micro API, Waters) with ionization electrospray (ESI), operating in positive mode.

1.8 Phytochemical Study of *Euphorbia pubescens*

Euphorbia pubescens Spreng. (Euphorbiaceae) was harvested in July 2015, in Sesimbra, Portugal, and identified by Dr. Teresa Vasconcelos of Instituto Superior de Agronomia, Universidade de Lisboa.

In Scheme 5 is depicted the process of extraction and fractionation of the plant, both of which were conducted by João Gomes (13). From this process eleven crude fractions were obtained (A to L) in accordance to the corresponding TLC that showed different compositions. In this work, just fractions A (1-8), B (9-20) and J (93-111) were studied.

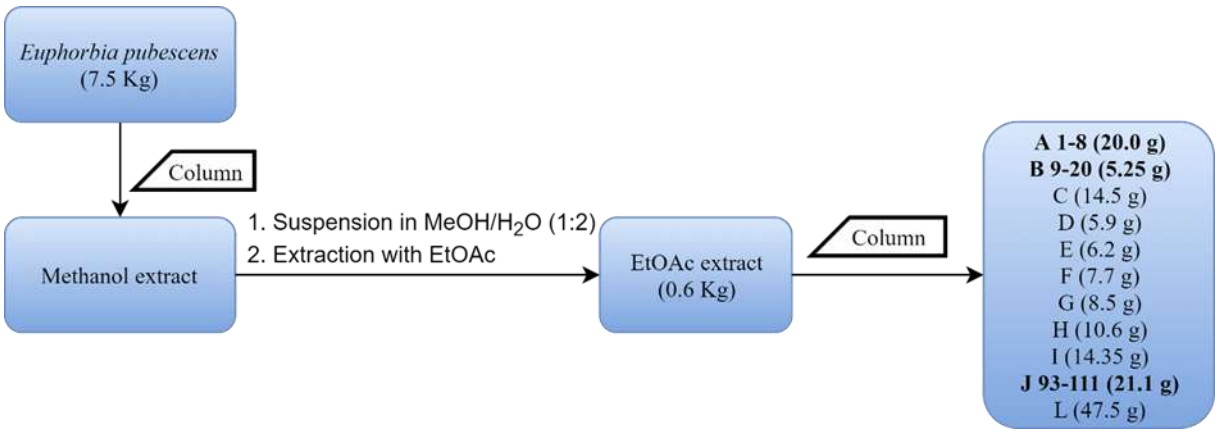

Scheme 5 *- Extraction and fractionation of E. pubescens.*

1.8.1 Study of fraction A (1-8) and B (9-20)

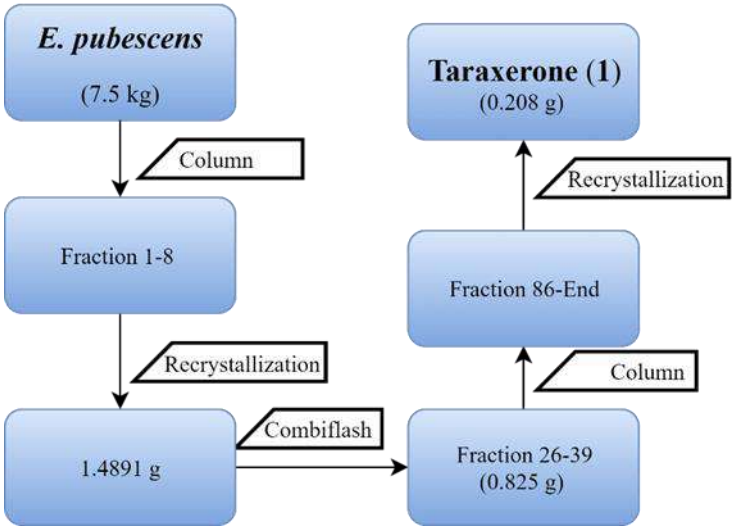

Scheme 6 *- Study of fraction A (1-8).*

Fraction A (1-8) (20.0 g, eluted with *n*-hexane/EtOAc 1:0 to *n*-hexane/EtOAc 8:2) was recrystallized from acetone to give 1.25 g of white crystals. These crystals were then submitted to a combiflash chromatography, with the most interesting fraction being 26-39 (0.285 g) that was further separated through column chromatography (*n*-hexane/EtOAc 1:0 to 0:1), obtaining fraction 86-End, the more interesting sub-fraction. By recrystallization of this sub-fraction, 0.208 g of compound **1** (taraxerone) was obtained (Scheme 6).

Taraxerone (1)

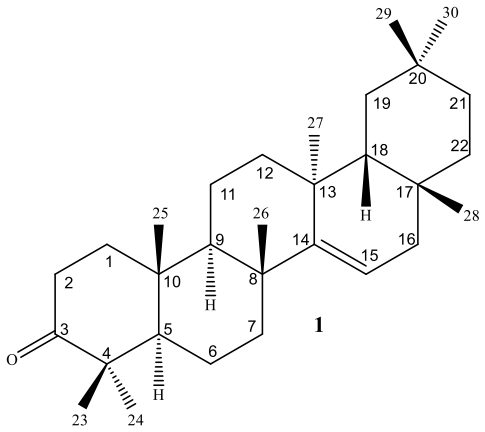

1

White crystals

m.p. 141-143 °C (Lit. 141 – 142ºC)(39)

$[\alpha]_D^{25}$ +50.0 ($CHCl_3$)

ν_{max}cm^{-1} (KBr): 2958 cm^{-1}, 2885 cm^{-1}, 2368 cm^{-1}, 1708 cm^{-1}

m/z 425 $[M+H]^+$

^{1}H NMR (300 MHz, $CDCl_3$): δ 5.56 (1H, *dd*, *J* = 8.2, 3.3 Hz, H-15), 1.14 (3H, *s*, H-27), 1.08 (3H, *s*, H-23), 1.08 (3H, *s*, H-25), 1.07 (3H, *s*, H-24), 0.95 (3H, *s*, H-29), 0.91 (6H, *s*, H-26, H-30), 0.83 (3H, *s*, H-28).

^{13}C NMR (75 MHz, $CDCl_3$): δ 217.70 (C-3), 157.77 (C-14), 117.35 (C-15), 55.94 (C-5), 48.96 (C-18), 48.86 (C-9), 47.73 (C-4), 40.80 (C-19), 39.03 (C-8), 38.51 (C-1), 37.90 (C-12), 37.85 (C-13), 37.70 (C-17), 36.83 (C-16), 35.93 (C-10), 35.26 (C-7), 34.29 (C-2), 33.73 (C-21), 33.51 (C-29), 33.24 (C-22), 30.07 (C-28), 30.01 (C-26), 30.01 (C-26), 28.95 (C-20), 26.27 (C-23), 25.72 (C-27), 21.63 (C-30), 21.50 (C-24), 20.12 (C-6), 17.60 (C-11), 14.96 (C-25).

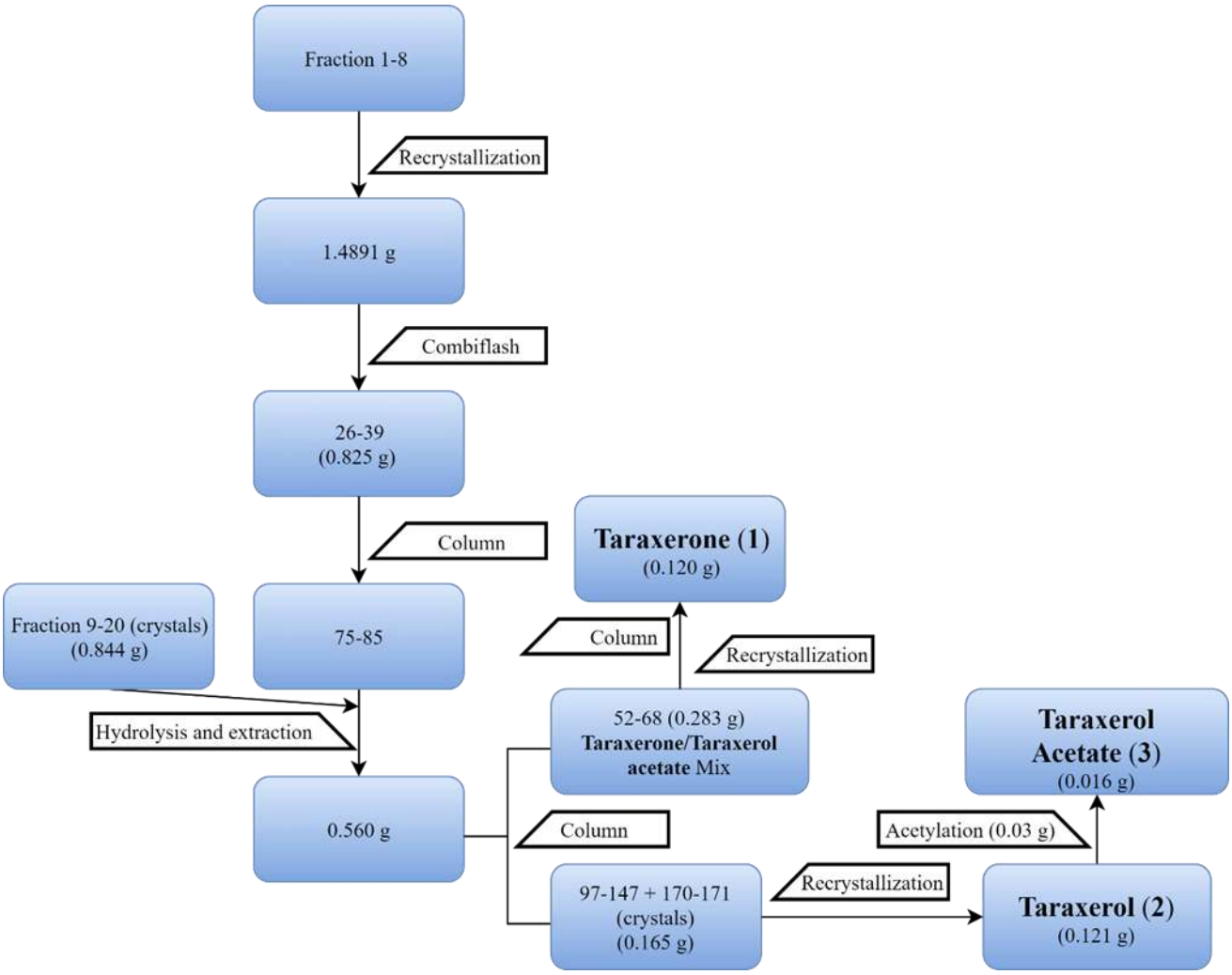

Scheme 7 *- Partial workup of fraction 1-8 and 9-20(crystals).*

Another sub-fraction of fraction A (1-8), sub-fraction 26-39 (0.82 g), was submitted to column chromatography (*n*-hexane/EtOAc 1:0 to 0:1), with the most interesting fraction of this column being 75-85. To fraction 75-85 were added the crystals of fraction B (9-20) (0.84 g – obtained by recrystallization with acetone). The mixture was submitted to hydrolysis (5% KOH in methanol, 25 mL, stirring at room temperature for 6 hours), after which it was diluted with water and exhaustively extracted with EtOAc. The organic layers were dried with anhydrous sodium sulphate, evaporated and the corresponding fraction (0.560g) was submitted to column chromatography eluted with mixtures of *n*-hexane/EtOAc of increasing polarity. Several fractions were obtained, the most important being 52-68 (0.263 g), from which 0.120 g of compound **1** was isolated, and fractions 97-147 that was added to the crystals of 170-171, and recrystallized, yielding 0.121 g of compound **2** (Taraxerol).

Compound **2** (0.03 g) was acetylated to yield 0.016 g of compound **3** (Taraxerol Acetate), which was already present in some fractions, usually with taraxerone, and showed itself difficult to separate (Scheme 7).

Taraxerol (2)

Amorphous white powder

$[\alpha]_D^{25}$ +79.8 ($CHCl_3$)

ν_{max}cm^{-1} (KBr): 3487 cm^{-1}

m/z 409 $[M+H-H_20]^+$

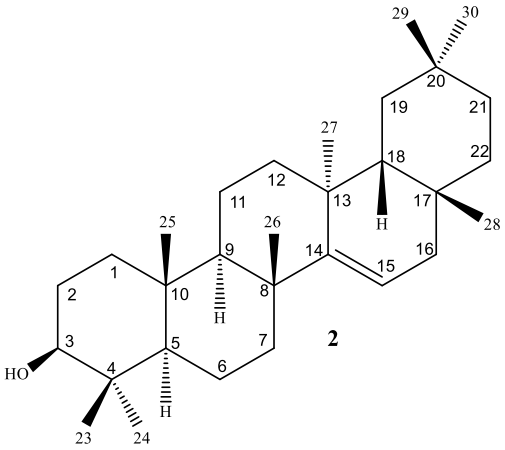

^{1}H NMR (300 MHz, $CDCl_3$): δ 5.53 (1H, *dd*, *J* = 8.2, 3.3 Hz, H-15), 3.19 (3H, *dd*, (*J* = 15.6, 5.4, H-3), 1.09 (3H, *s*, H-27), 0.98 (3H, *s*, H-23), 0.95 (3H, *s*, H-29), 0.93 (3H, *s*, H-24), 0.91 (6H, *s*, H-26, H-30), 0.82 (3H, *s*, H-28), 0.80 (3H, *s*, H-25).

^{13}C NMR (75 MHz, $CDCl_3$): δ 158.25 (C-14), 117.03 (C-15), 79.23 (C-3), 55.69 (C-5), 49.44 (C-18), 48.92 (C-9), 41.49 (C-19), 39.14 (C-8), 38.92 (C-4), 38.16 (C-1), 37.90 (C-10), 37.87 (C-13), 37.73 (C-17), 36.84 (C-16), 35.94 (C-12), 35.28 (C-7), 33.86 (C-21), 33.51 (C-29), 33.26 (C-22), 30.08 (C-26), 29.98 (C-28), 28.95 (C-20), 28.15 (C-23), 27.31 (C-2), 26.06 (C-27), 21.47 (C-30), 18.95 (C-6), 17.66 (C-11), 15.60 (C-25), 15.58 (C-24).

Taraxerol acetate (3)

Amorphous white powder

$[\alpha]_D^{25}$ +55.5 ($CHCl_3$)

ν_{max}cm^{-1} (KBr): 1724 cm^{-1}, 1252 cm^{-1}

m/z 409 $[M+H-C_2H_4O_2]^+$

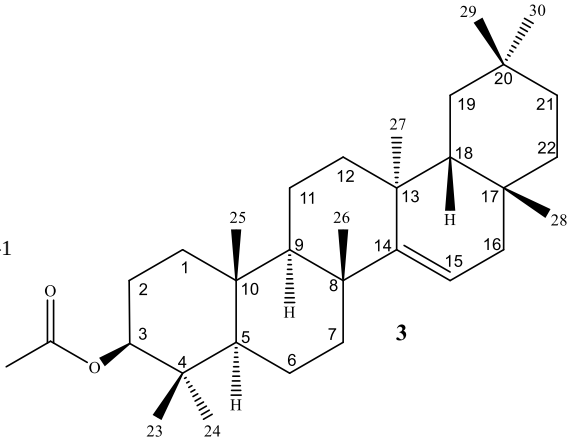

^{1}H NMR (300 MHz, $CDCl_3$):δ 5.53 (1H, *dd*, *J* = 8.1, 3.2 Hz, H-15), 4.46 (3H, *dd*, *J* = 9.8, 6.2, H-3), 2.04 (3H, *s*, CO$\underline{CH_3}$), 1.09 (3H, *s*, H-26), 0.95 (6H, *s*, H-23, H-29), 0.90 (6H, *s*, H-25, H-30), 0.87 (3H, *s*, H-27), 0.86 (3H, *s*, H-28), 0.82 (3H, *s*, H-24).

^{13}C NMR (75 MHz, $CDCl_3$): δ 171.12 (<u>CO</u>CH_3), 158.14 (C-14), 117.09 (C-15), 81.17 (C-3), 55.80 (C-5), 49.35 (C-18), 48.93 (C-9), 41.38 (C-19), 39.14 (C-4), 38.05 (C-8), 37.84 (C-1/C-10), 37.71 (C-17), 37.55 (C-13), 36.82 (C-16), 35.93 (C-12), 35.27 (C-7), 33.83 (C-21), 33.49 (C-29), 33.25 (C-22), 31.06 (C-26), 30.07 (C-28), 29.98 (C-20), 28.95 (C-2), 28.13 (C-23), 26.07 (C-27), 23.61 (C-30), 21.43 (CO<u>CH</u>$_3$), 18.84 (C-6), 17.66 (C-11), 16.73 (C-25), 15.64 (C-24).

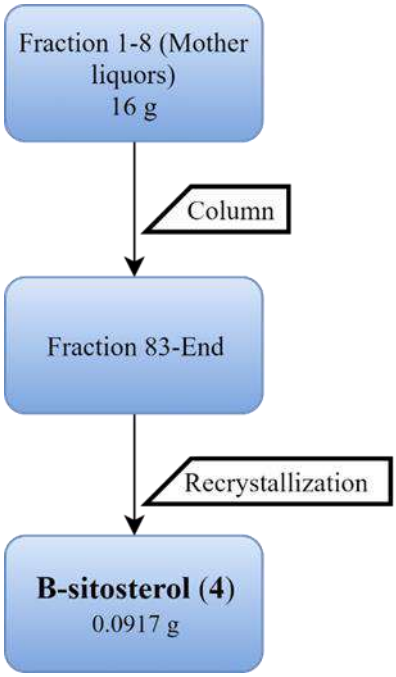

Scheme 8 *- Workup of fraction 83-End of fraction 1-8 (Mother liquors).*

After the recrystallization of fraction 1-8, the mother liquors were also studied and submitted to column chromatography (*n*-hexane/EtOAc 1:0 to 0:1), with the fractions 21 and 83-End being of interest and recrystallized. This led to the isolation of 0.0917 g of compound **4** (β-sitosterol) from sub-fraction 83-End (Scheme 8).

β-sitosterol (4)

White powder

m.p. 130-131 °C (Lit. 128 – 130ºC)(49)

$[\alpha]_D^{25}$ -15.9 ($CHCl_3$)

ν_{max}cm^{-1} (KBr): 3425 cm^{-1}

m/z 397 $[M+H-H_2O]^+$

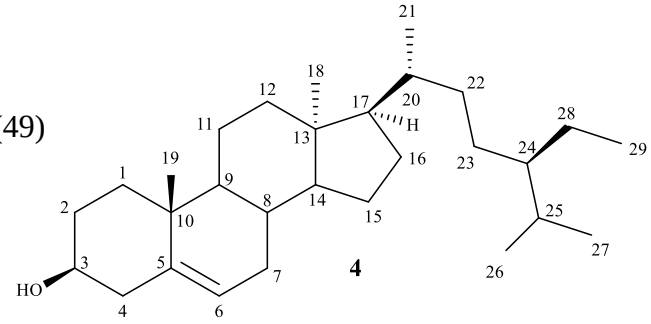

^{1}H NMR (300 MHz, $CDCl_3$):δ 5.35 (1H, *d*, *J* = 5.4 Hz, H-6), 3.52 (1H, *m*, H-3), 1.01 (3H, *s*, H-19), 0.92 (3H, *d*, *J* = 6.5 Hz, H-21), 0.86 (3H, *t*, *J* = 13.6, 7.2 Hz, H-29), 0.83 (3H, *d*, *J* = 6.5 Hz, H-27), 0.80 (3H, *d*, *J* = 6.6 Hz, H-26), 0.68 (3H, *s*, H-18).

^{13}C NMR (75 MHz, $CDCl_3$):δ 149.93 (C-5), 121.67 (C-6), 71.77 (C-3), 56.73 (C-14), 56.23 (C-17), 50.31 (C-9), 46.02 (C-22), 42.49 (C-13), 42.27 (C-4), 39.79 (C-12), 37.42 (C-1), 36.67 (C-10), 36.30 (C-18), 34.12 (C-20), 32.08 (C-7), 31.85 (C-2), 31.64 (C-8), 29.13 (C-25), 28.20 (C-16), 26.26 (C-15), 26.06 (C-21), 23.24 (C-23), 21.04 (C-11), 19.76 (C-26), 19.35 (C-27), 18.99 (C-19), 18.73 (C-28), 11.93 (C-24), 11.81 (C-29).

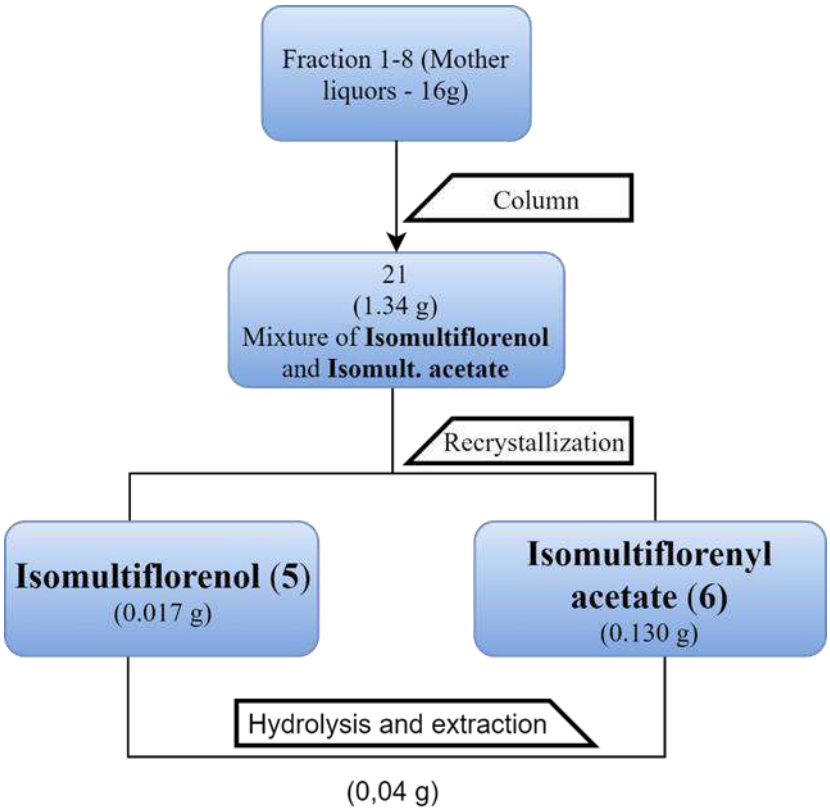

***Scheme 9** - Workup of fraction 21 of fraction 1-8 (Mother liquors).).*

Fraction 21 (1.34 g) was also recrystallized (EtOAc/*n*-hexane) to obtain 130 mg of compound **5** and a mixture of compounds **5** (isomultiflorenol) and **6** (isomultiflorenyl acetate). As compound **6** was not able to be isolated for a correct characterization, 40 mg of compound **5** were submitted to hydrolysis (25mL MeOH /KOH 5%, stirring at room temperature for 6 hours). The reaction mixture was suspended in H_2O and extracted several times with EtOAc, yielding 0.017 g of isolated compound **6** (Scheme 9).

Isomultiflorenol (5)

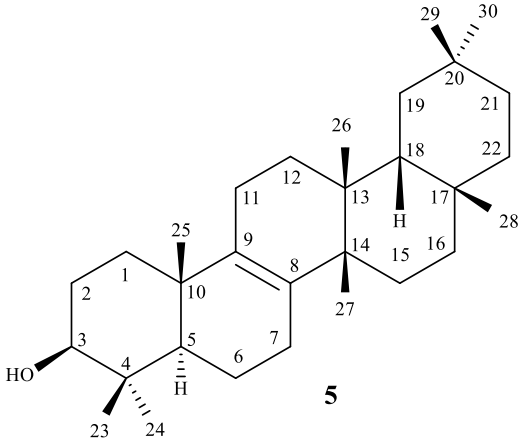

5

Amorphous white powder

$[\alpha]_D^{25}$ +88.3 ($CHCl_3$)

ν_{max}cm^{-1} (KBr): 3410 cm^{-1}, 1458 cm^{-1}, 1379 cm^{-1}

m/z 409 $[M+H-H_2O]^+$

^{1}H NMR (300 MHz, $CDCl_3$): δ 3.23 (1H, *dd*, *J* = 11.4, 4.8 Hz, H-3), 1.07 (3H, *s*, H-28), 1.06 (3H, *s*, H-26), 1.00 (3H, *s*, H-30), 0.99 (3H, *s*, H-29), 0.97 (3H, *s*, H-27), 0.96 (6H, *s*, H-25, H-24), 0.80 (3H, *s*, H-23).

^{13}C NMR (75 MHz, $CDCl_3$): δ 135.24 (C-8), 133.67 (C-9), 79.18 (C-3), 50.86 (C-5), 44.27 (C-18), 41.14 (C-14), 38.96 (C-4), 37.77 (C-10), 37.44 (C-13), 36.96 (C-22), 36.85 (C-16), 35.20 (C-21), 34.66 (C-29), 34.55 (C-19), 34.34 (C-1), 33.14 (C-30), 31.65 (C-28), 30.95 (C-17), 30.84 (C-12), 28.48 (C-20), 28.20 (C-23), 28.08 (C-7), 27.65 (C-15), 26.41 (C-27), 24.84 (C-2), 20.96 (C-11), 19.97 (C-25), 19.39 (C-6), 19.12 (C-26), 15.76 (C-24).

Isomultiflorenyl acetate (6)

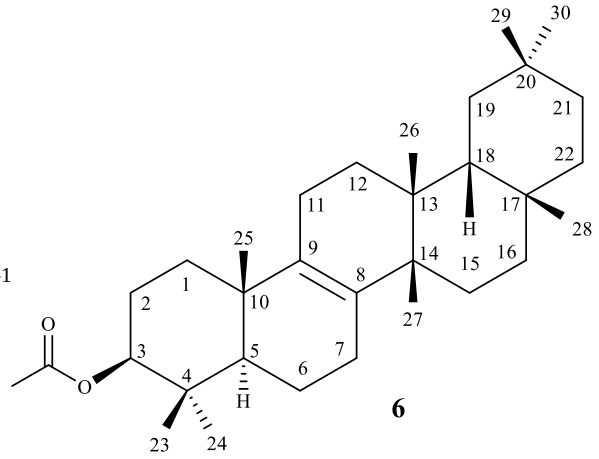

6

Amorphous white powder

$[\alpha]_D^{25}$ +98.8 ($CHCl_3$)

ν_{max}cm^{-1} (KBr): 1726 cm^{-1}, 1250 cm^{-1}

m/z 409 $[M+H-C_2H_4O_2]^+$

^{1}H NMR (300 MHz, $CDCl_3$): δ 4.48 (1H, *dd*, *J* = 11.3, 6.5 Hz, H-3), 2.05 (3H, *s*, COC<u>H</u>$_3$), 1.07 (3H, *s*, H-28), 1.05 (3H, *s*, H-27), 0.97 (9H, *s*, H-25, H-26, H-30), 0.95 (3H, *s*, H-29), 0.88 (3H, *s*, H-24), 0.87 (3H, *s*, H-23).

^{13}C NMR (75 MHz, $CDCl_3$): δ 171.25 (<u>CO</u>CH_3), 135.23 (C-8), 133.45 (C-9), 81.10 (C-3), 50.87 (C-5), 44.23 (C-18), 43.11 (C-21), 41.11 (C-14), 37.84 (C-4), 37.56 (C-10), 37.35 (C-13), 36.83 (C-16), 36.81 (C-22), 34.76 (C-1), 34.45 (C-29), 34.31 (C-19), 33.07 (C-30), 31.63 (C-28), 30.90 (C-17), 30.74 (C-12), 28.45 (C-20), 28.11 (C-24), 27.46 (C-7), 26.30 (C-

15), 24.74 (C-27), 24.32 (C-2), 21.49 ($CO\underline{CH_3}$), 20.94 (C-11), 20.00 (C-25), 19.20 (C-6), 19.04 (C-26), 16.83 (C-23).

1.8.2 Study of fraction J (93-111)

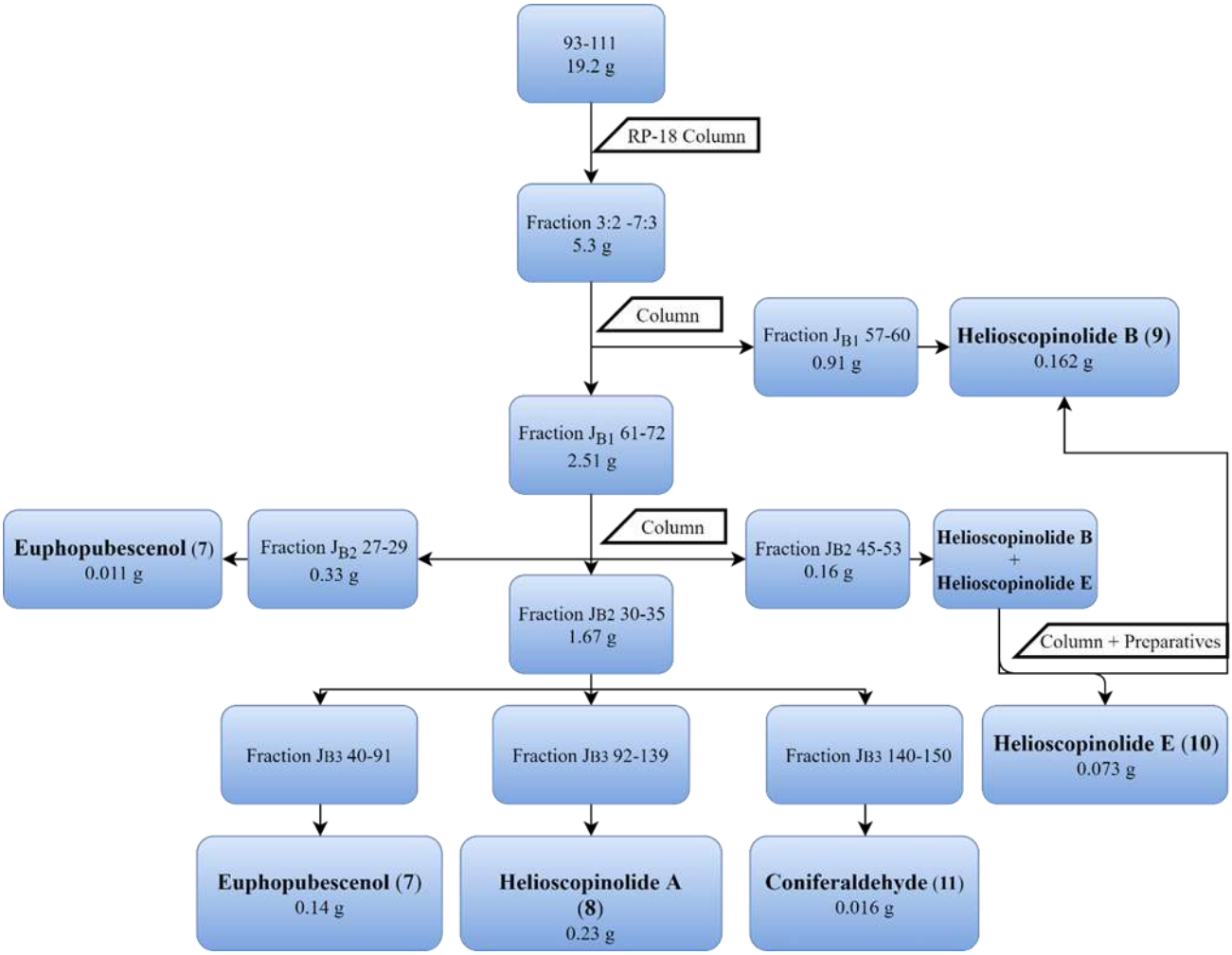

Scheme 10 *- Workup of fraction J (93-111).*

Fraction J (93-111) (19.2g, eluted with *n*-hexane/EtOAc 7:3) went through reverse-phase chromatography (MeOH/H_2O 1:1 to MeOH/H_2O 1:0 in increasing gradients of 10%). After TLC monitoring, the fractions with similar profile were combined (Scheme 10).

From this, fractions eluted with mixtures of MeOH/H_2O 3:2 – 7:3 were chosen to be studied and associated.

The referred fraction (5.3 g) was submitted to CC using *n*-hexane/EtOAc (1:0 up to 4:1). According to differences in composition as indicated by TLC, seven crude fractions were obtained (Fractions J_B).

Fraction J_{B1} (57-60) (0.91 g) was separated on a CombiFlash® Rf System (24 g, flash column, RediSepRf) with *n*-hexane-EtOAc (1:0 to 0:1, used in increasing gradients of 5%; 5 ml/min). To obtain helioscopinolide B (**9**), a subfraction was recrystallized with EtOAc/*n*-hexane yielding 115 mg of pure compound.

Fraction J_{B1} (61-72) (2.51 g, *n*-hexane/EtOAc 3:2) was chromatographed on a Combiflash system (120 g, flash column, RediSepRf) with *n*-hexane-EtOAc (1:0 to 0:1, used in increasing gradients of 5%; 7 ml/min) and yielded three interesting fractions: J_{B2} 27-29 (0.33 g), J_{B2} 30-35 (1.67 g) and J_{B2} 45-53 (0.16 g).

Fraction J_{B2} 27-29 was submitted to a chromatographic column using 100g of SiO_2 and eluted with mixtures of CH_2Cl_2-MeOH of increasing polarity to give, 11 mg of compound **7** (euphopubescenol). Fraction J_{B2} 30-35 was submitted to column chromatography (CH_2Cl_2/acetone 1:0 to 4:1), yielding three interesting fractions, J_{B3} 40-91, J_{B3} 92-139 and J_{B3} 140-150. Fraction J_{B3} 40-91 was again submitted to CC with similar eluent, yielding 0.14 g of the already isolated compound **7** (euphopubescenol). Fraction J_{B3} 92-139 was recrystallized to give 0.23 g of helioscopinolide A (**8**). Fraction J_{B3} 140-150 was further purified by preparative chromatography yielding 16 mg of coniferaldehyde (**11**).

Fraction J_{B2} 45-53(0.16 g) was submitted to column chromatography (SiO_2), using as eluents mixtures of hexane/EtOAc (1:0 to 0:1), and a mixture of helioscopinolide B (**9**) and E (**10**) was collected. This mixture was then submitted to preparative chromatography with the successful isolation of 73 mg of helioscopinolide E and 47 mg of helioscopinolide B.

Euphopubescenol (7)

Amorphous white powder

$[\alpha]_D^{25}$ +74.6 ($CHCl_3$)

ν_{max}cm^{-1} (KBr): 3520 cm^{-1}, 1748 cm^{-1}, 1715 cm^{-1}, 1633 cm^{-1}

m/z 553 [M+H-CH_3COOH]$^+$

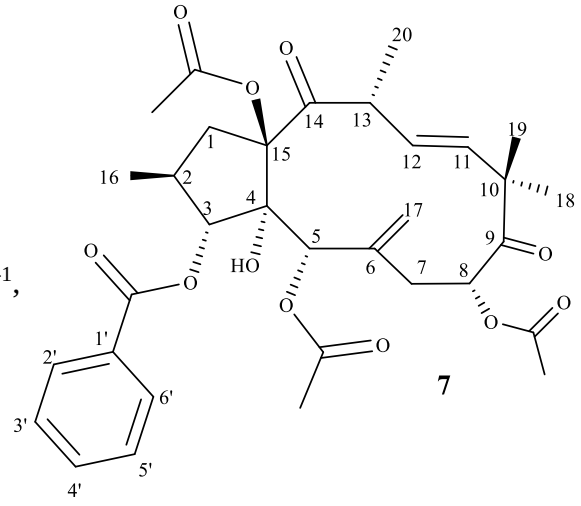

7

^{1}H NMR (300 MHz, $CDCl_3$):δ 7.97 (2H, *dd*, *J* = 8.0, 1.5 Hz, Bz (H-2',H-6')), 7.57 (1H, *tt*, *J* = 7.5, 1.5 Hz, Bz (H-4')), 7.42 (2H, *t*, *J* = 7.8 Hz, Bz (H-3',H-5')), 5.92 (1H, *dd*, *J* = 16.0, 9.0 Hz, H-12), 5.89 (1H, *d*, *J* = 9.0 Hz, H-11) 5.67 (1H, *d*, *J* = 8.9 Hz, H-8), 5.61 (1H, *d*,

J = 10.5 Hz, H-3), 5.12 (2H, *s*, H-7), 4.86 (1H, *s*, H-5), 3.85 (1H, *m*, H-13), 2.91 (1H, *tdd*, *J* = 10.4, 7.0, 3.5 Hz, H-2), 2.43 (2H, *m*, H-1α /1β), 2.16 (3H, *s*, 15-O(CO$\underline{CH_3}$)), 2.08 (3H, *s*, 5-O(CO$\underline{CH_3}$)), 2.00 (1H, *s*, H-7β), 1.91 (3H, *s*, 8-O(CO$\underline{CH_3}$)), 1.71 (1H, *dd*, *J* = 14.9; 9.2, H7-α), 1.46 (3H, *s*, H-19), 1.38 (3H, *d*, *J* = 6.5 Hz, H-20), 1.24 (3H, *d*, *J* = 6.9 Hz, H-16), 1.22 (3H, *s*, H-18)).

^{13}C NMR (75 MHz, $CDCl_3$):δ 208.20 (C-9), 204.61 (C-14), 169.87 (8-O ($\underline{CO}CH_3$)), 168.86 (15-O ($\underline{CO}CH_3$)), 168.42 (5-O ($\underline{CO}CH_3$)), 166.60 (3-OBz), 140.17 (C-6), 136.91 (C-11), 133.70 (Bz (4')), 132.84 (C-12), 130.19 (Bz (2', 6')), 129.09 (Bz (1')), 128.53 (Bz (3', 5')), 116.89 (C-17), 94.62 (C-15), 82.94 (C-4), 77.89 (C-3), 73.28 (C-5), 72.41 (C-8), 50.66 (C-10), 46.91 (C-13), 38.82 (C-1), 36.90 (C-2), 35.97 (C-7), 24.57 (C-18, C-19), 21.14 (15-O (CO$\underline{CH_3}$)), 20.71 (5-O (CO$\underline{CH_3}$)), 20.42 (8-O (CO$\underline{CH_3}$)), 20.16 (C-20), 17.79 (C-16).

Helioscopinolide A (8)

White crystals

m.p. 204-206 °C (Lit. 205 ºC) (13)

$[\alpha]_D^{25}$ +587.4 ($CHCl_3$)

ν_{max}cm^{-1} (KBr): 3478 cm^{-1}, 1734 cm^{-1}, 1398 cm^{-1}

m/z 317 $[M+H]^+$

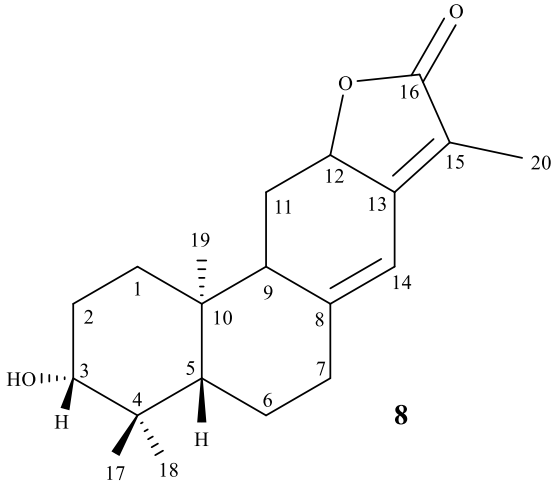

8

^{1}H NMR (300 MHz, $CDCl_3$): δ 6.27 (1H, *s*, H-14), 4.85 (1H, *ddd*, *J* = 13.6, 6.2, 1.8 Hz, H-12), 3.27 (1H, *dd*, *J* = 11.6, 4.4 Hz, H-3), 2.53 (2H, *m*, H-11), 2.18 (1H, *dd*, *J* = 15.1, 9.0 Hz, H-9), 1.94 (2H, *dt*, *J* = 13.1, 3.6 Hz, H-1), 1.81 (3H, *d*, *J* = 1.7 Hz, H-20), 1.64 (2H, *m*, H-2), 1.14 (1H, *dd*, *J* = 12.5, 2.5 Hz, H-5), 1.02 (3H, *s*, H-17), 0.92 (3H, *s*, H-19), 0.81 (3H, *s*, H-18).

^{13}C NMR (75 MHz, $CDCl_3$): δ 175.39 (C-16), 156.17 (C-13), 151.58 (C-8), 116.61 (C-15), 114.31 (C-14), 78.66 (C-3), 76.00 (C-12), 54.48 (C-5), 51.67 (C-9), 41.34 (C-10), 39.21 (C-4), 37.53 (C-1), 37.04 (C-7), 28.79 (C-17), 27.70 (C-2), 27.66 (C-11), 23.56 (C-6), 16.82 (C-19), 15.71 (C-18), 8.37 (C-20).

Helioscopinolide B (9)

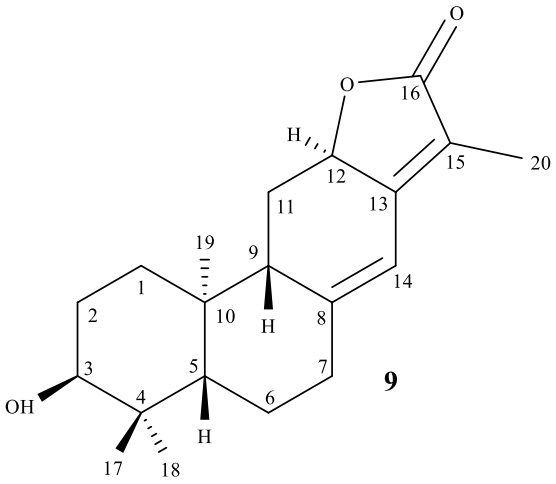

9

Colorless oil

$[\alpha]_D^{25}$ +417.6 ($CHCl_3$)

ν_{max}cm^{-1} (KBr): 3467 cm^{-1}, 1730 cm^{-1}, 1393 cm^{-1}

m/z 317 $[M+H]^+$

^{1}H NMR (300 MHz, $CDCl_3$): 6.25 (1H, *s*, H-14), 4.86 (1H, *ddd*, J = 13.3, 6.1, 1.2, H-12), 3.46 (1H, *d*, J = 3.2, H-3), 2.56 (1H, *m*, H-11), 2.47 (1H, *dd*, J = 4.2, 2.3, H-7), 2.29 (1H, *d*, J = 8.7, H-9), 1.81 (3H, *d*, J = 1.3, H-20), 1.60-1.70 (4H, *m*, H-1, H-2), 1.64 (1H, *m*, H-5), 1.41 (2H, *m*, H-6), 0.98 (3H, *s*, H-17), 0.93 (3H, *s*, H-19), 0.86 (3H, *s*, H-18).

^{13}C NMR (75 MHz, $CDCl_3$): 175.45 (C-16), 156.30 (C-13), 152.23 (C-8), 116.37 (C-15), 114.12 (C-14), 76.12 (C-12), 75.62 (C-3), 51.64 (C-9), 48.41 (C-5), 41.39 (C-10), 37.85 (C-4), 37.14 (C-7), 32.19 (C-1), 28.83 (C-17), 27.56 (C-11), 25.81 (C-2), 23.49 (C-6), 22.33 (C-18), 16.81 (C-19), 8.33 (C-20).

Helioscopinolide E (10)

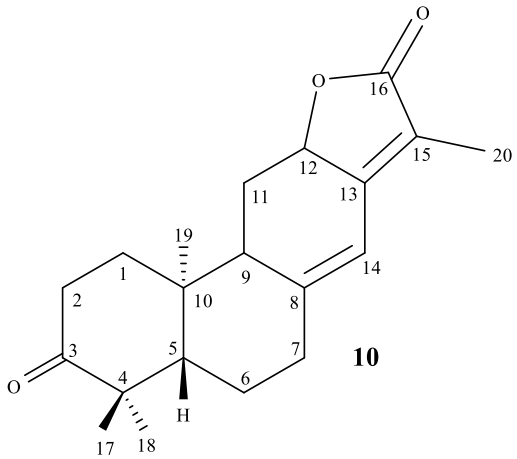

10

Colorless oil

$[\alpha]_D^{25}$ +395.9 ($CHCl_3$)

ν_{max}cm^{-1} (KBr): 1706 cm^{-1}, 1751 cm^{-1}

m/z 315 $[M+H]^+$

^{1}H NMR (300 MHz, $CDCl_3$): 6.33 (1H, *s*, H-14), 4.87 (1H, *ddd*, J = 13.3, 6.1, 1.8, H-12), 2.56 (1H, *m*, H-2), 2.22 (4H, *m*, H-1, H-7), 1.84 (3H, *d*, J = 1.6, H-20), 1.59 (5H, *m*, H-5, H-6, H-11), 1.13 (3H, *s*, H-17), 1.08 (3H, *s*, H-19), 1.05 (3H, *s*, H-18).

^{13}C NMR (75 MHz, $CDCl_3$): 215.63 (C-3), 175.17 (C-16), 155.65 (C-13), 155.65 (C-13), 150.30 (C-8), 117.87 (C-15), 114.87 (C-14), 75.75 (C-12), 50.80 (C-9), 47.67 (C-4), 45.90

(C-5), 41.06 (C-10), 37.53 (C-1), 36.73 (C-7), 34.53 (C-2), 27.94 (C-11), 26.66 (C-17), 24.74 (C-6), 21.93 (C-18), 16.38 (C-19), 8.45 (C-20).

Coniferaldehyde (11)

Amorphous light-brown powder

ν_{max}cm^{-1} (KBr): 3357 cm^{-1},1691 cm^{-1}, 1618 cm^{-1}

m/z 179 [M+H]$^{+}$

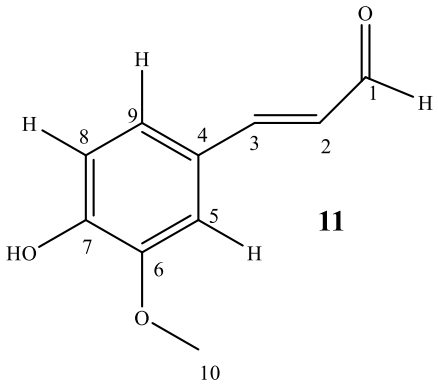

11

^{1}H NMR (300 MHz, CDCl$_3$): 9.65 (1H, *d*, *J* = 7.7, H-1), 7.42 (1H, *d*, *J* = 15.7, H-3), 7.12 (1H, *dd*, *J* = 8.3, 2.0, H-9), 7.07 (1H, *d*, *J* = 1.9, H-5), 6.96 (1H, *d*, *J* = 8.1, H-8), 6.59 (1H, *dd*, *J* = 15.8, 7.7, H-2), 3.94 (3H, *s*, H-10).

^{13}C NMR (75 MHz, CDCl$_3$): 193,77 (C-1), 153,24 (C-3), 149,12 (C-7), 147,12 (C-6), 126,80 (C-4), 126,57 (C-2), 124,20 (C-9), 115,10 (C-8), 109,64 (C-5), 56,15 (C-10).

1.8.3 Derivatization of taraxerone (**1**)

Taraxerone was derivatized by reaction with three different hydrazines: phenylhydrazine (reaction **1.1**), hydrazine monohydrate (reaction **1.2**) and 2,4-dinitrophenylhydrazine (reaction **1.3**). These reactions involved the mixture of 30 mg of taraxerone with approximately 5 equivalents of the corresponding reagent (40 µL for **1.1**, 20 µL for **1.2** and 60 mg for **1.3**), using methanol and dichloromethane (3:2, 10 mL) as solvent , with the addition of 200 µL of a solution of acetic acid 10%, occurring overnight, under reflux.

The compounds were purified through column chromatography (SiO2), using as eluent mixtures of *n*-hexane/EtOAc (1:0 to 0:1), as is the case with **1.3** (34 mg of product, with a yield of 79%), or through preparative chromatography, as is the case with **1.1** (22 mg of product, with a yield of 61%) and **1.2** (13.3 mg of product, with a yield of 42%).

Compound 1.1

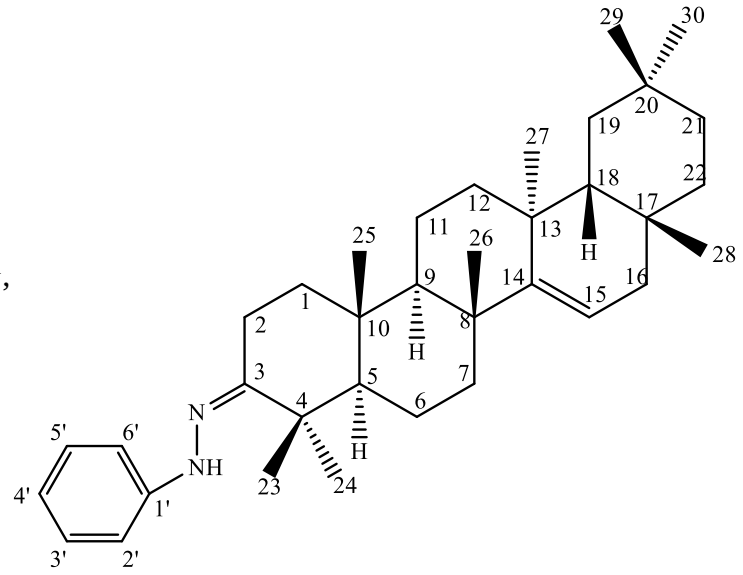

Yellow amorphous solid

$[\alpha]_D^{25}$ +225.9 ($CHCl_3$)

ν_{max}cm^{-1} (KBr): 3664 cm^{-1}, 1631 cm^{-1}, 684 cm^{-1}

m/z 513 $[M+H]^+$

^{1}H NMR (300 MHz, $CDCl_3$): δ 7.72 (1H, *m*, H-4'), 7.49 (4H, *dd*, *J* = 5.1, 2.0 Hz, H-2', H-3', H-5', H-6'), 5.54 (1H, *dd*, *J* = 8.1, 3.2 Hz, H-15), 1.14 (3H, *s*, H-27), 1.09 (3H, *m*, H-24), 1.07 (3H, *s*, H-25), 0.96 (3H, *s*, H-29), 0.95 (3H, *s*, H-26), 0.92 (3H, *s*, H-30), 0.84 (3H, *s*, H-28).

^{13}C NMR (75 MHz, $CDCl_3$): δ 158.15 (C-14), 151.11 (C-3), 131.32 (C-1'), 129.31 (C-3', C-5'), 122.76 (C-4'), 117.02 (C-15), 107.29 (C-2', C-6'), 51.74 (C-5), 48.95 (C-18), 48.86 (C-9), 42.50 (C-4), 41.25 (C-19), 39.23 (C-8), 38.27 (C-1), 37.88 (C-12), 37.71 (C-13), 36.86 (C-17), 35.95 (C-16), 35.30 (C-10), 34.00 (C-7), 33.93 (C-2), 33.51 (C-29), 33.28 (C-21), 30.10 (C-22), 30.01 (C-28), 28.97 (C-26), 26.22 (C-20), 23.16 (C-23), 22.42 (C-27), 21.49 (C-30), 21.43 (C-24), 18.78 (C-6), 17.61 (C-11), 15.70 (C-25).

Compound 1.2

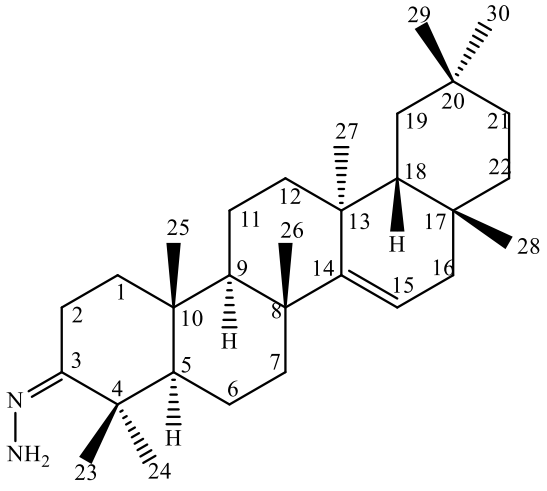

White amorphous solid

$[\alpha]_D^{25}$ +19.1 ($CHCl_3$)

ν_{max}cm^{-1} (KBr): 3490 cm^{-1}, 1638 cm^{-1}

m/z 439 $[M+H]^+$

^{1}H NMR (300 MHz, $CDCl_3$): δ 5.55 (1H, *dd*, *J* = 8.3, 3.4 Hz, H-15), 1.21 (3H, *s*, H-27),1.11 (3H, *s*, H-25), 1.04 (3H, *s*, H-24), 0.95 (3H, *s*, H-29), 0.91 (3H, *s*, H-26), 0.89 (3H, *s*, H-30), 0.83 (3H, *s*, H-28).

^{13}C NMR (75 MHz, $CDCl_3$): δ 158.08 (C-14), 148.31 (C-3), 117.13 (C-15), 56.35 (C-5), 49.07 (C-18), 48.95 (C-9), 41.80 (C-4), 41.11 (C-19), 39.12 (C-8), 38.25 (C-1), 38.08 (C-12), 37.86 (C-13), 37.70 (C-17), 36.83 (C-16), 35.93 (C-10), 35.27 (C-7), 33.51 (C-29), 33.25 (C-22), 30.08 (C-28), 30.01 (C-26), 28.95 (C-20), 27.80 (C-2), 25.84 (C-21), 23.67 (C-23), 23.43 (C-30), 21.47 (C-24), 20.00 (C-6), 17.91 (C-27), 17.60 (C-11), 15.06 (C-25).

Compound 1.3

Orange amorphous solid

$[\alpha]_D^{25}$ +13.3 ($CHCl_3$)

ν_{max}cm^{-1} (KBr): 3325 cm^{-1},1620 cm^{-1}, 1541 cm^{-1}, 1520 cm^{-1}

m/z 605 $[M+H]^+$

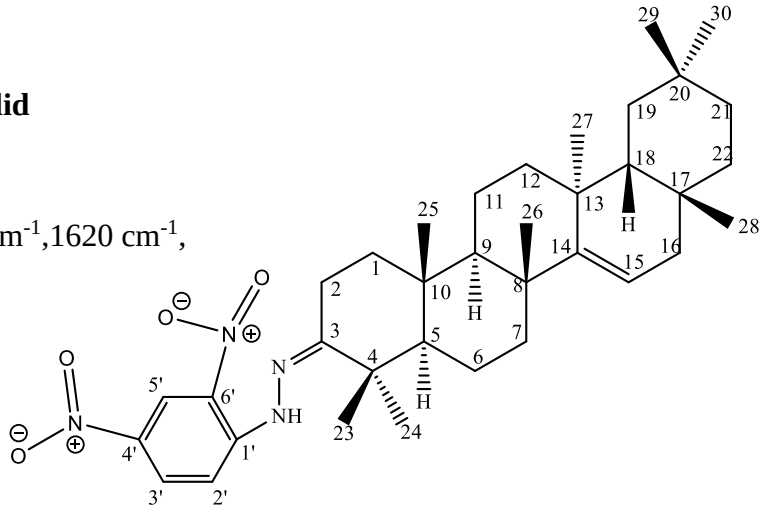

^{1}H NMR (300 MHz, $CDCl_3$): δ 9.12 (1H, *d*, *J* = 2.5 Hz, H-5'), 8.29 (1H, *dd*, *J* = 9.6, 2.6 Hz, H-3'), 7.95 (1H, *d*, *J* = 9.6 Hz, H-2'), 5.56 (1H, *dd*, *J* = 8.2, 3.2 Hz, H-15), 1.18 (3H, *s*, H-25), 1.15 (3H, *s*, H-27), 1.07 (3H, *s*, H-24), 0.95 (3H, *s*, H-29), 0.92 (3H, *s*, H-30), 0.90 (3H, *s*, H-26), 0.83 (3H, *s*, H-28).

^{13}C NMR (75 MHz, $CDCl_3$): δ 167.31 (C-3), 157.77 (C- 14), 145.77 (C-4'), 137.65 (C-1'), 130.10 (C-6'), 129.11 (C-3'), 123.75 (C-2'), 117.36 (C-15), 116.64 (C-5'), 56.12 (C-5), 48.95 (C-18), 48.83 (C-9), 42.49 (C-4), 40.91 (C-19), 39.06 (C-8), 38.00 (C-1), 37.85 (C-12), 37.68 (C-13), 37.56 (C-17), 36.83 (C-16), 35.94 (C-10), 35.26 (C-7), 33.71 (C-21), 33.50 (C-29), 33.23 (C-22), 30.07 (C-28), 30.01 (C-26), 28.94 (C-20), 28.54 (C-2), 25.78 (C-23), 24.25 (C-27), 21.49 (C-30), 20.65 (C-24), 20.17 (C-6), 17.63 (C-11), 14.79 (C-25).

References

1. Mwine JT, Damme P Van. Why do Euphorbiaceae tick as medicinal plants? A review of Euphorbiaceae family and its medicinal features. J Med Plant Res. 2011;5(5):652–62.
2. Molnár J, Hohmann J, Vasas A, Rédei D. Diterpenes from European Euphorbia Species Serving as Prototypes for Natural-Product-Based Drug Discovery. European J Org Chem. 2012;1–17.
3. Shi Q, Su X, Kiyota H. Chemical and Pharmacological Research of the Plants in Genus Euphorbia. Chemical Rev. 2008;108(10):4295–327.
4. Ogunlesi M, Okiei W, Ofor E, Osibote AE. Analysis of the essential oil from the dried leaves of *Euphorbia hirta* Linn (Euphorbiaceae), a potential medication for asthma. African J Biotechnol. 2009;8(24):7042–50.
5. Kim SJ, Jang YW, Hyung KE, Lee DK, Hyun KH, Park S, et al. Therapeutic Effects of Methanol Extract from *Euphorbia kansui* Radix on Imiquimod-Induced Psoriasis. J Immunol Res. 2017;2017:17.
6. Ahmed S, Fatima L. Pharmacological actions and therapeutic benefits of thuhar (*Euphorbia neriifolia*): A review. Pharma Innov J. 2018;7(9):221–6.
7. Bani S, Kaul A, Khan B, Kumar V, Kumar N, Avtar K, et al. Anti-arthritic activity of a biopolymeric fraction from *Euphorbia tirucalli*. J Ethnopharmacol. 2007;110:92–8.
8. Tholl D. Biosynthesis and Biological Functions of Terpenoids in Plants. Adv Biochem Eng Biotechnol (2015) 148: 63–106.
9. Ashour M, Wink M, Gershenzon J. Biochemistry of terpenoids: monoterpenes, sesquiterpenes and diterpenes. Annual Plant Reviews. 2010;40:258–303.
10. Miziorko HM. Enzymes of the mevalonate pathway of isoprenoid biosynthesis. Arch Biochem Biophys. 2011;505(2):131–43.
11. Dewick PM. Medicinal Natural Products: A Biosynthetic Approach, 3rd Edition. 2009.
12. Hunter WN. The Non-mevalonate Pathway of Isoprenoid Precursor. J Biol Chem. 2007;282(30):21573–7.
13. Gomes JN da S. Development of a small library of bioactive compounds through isolation and molecular derivatization. Universidade de Lisboa, Faculdade de Farmácia; 2017.
14. Li J, Wang W, Song W, Xuan L. Fitoterapia (19αH)-lupane and (9βH)-lanostane triterpenes from *Euphorbia helioscopia* trigger apoptosis of tumor cell. Fitoterapia.

2018;125:24–32.

15. Ferreira RJ, Kincses A, Gajdács M, Spengler G, Santos DJVA dos, Molnár J, et al. Terpenoids from *Euphorbia pedroi* as Multidrug-Resistance Reversers. J Nat Prod. 2018;81:2032–40.
16. Banjar MFS, Mohamed GA, Shehata IA, Abdallah HM, Shati AA, Alfaifi MY, et al. Cycloschimperols A and B, new cytotoxic cycloartane triterpenoids from *Euphorbia schimperi*. Phytochem Lett. 2019;32:90–5.
17. Benabdelaziz I, Gómez-ruiz S, Benkhaled M, Carralero S, Schenker P, Salm A, et al. New cycloartane-type ester triterpenes from *Euphorbia pterococca* and biological evaluation. Fitoterapia. 2018;127:271–8.
18. Rozimamat R, Kehrimen N, Gao J, Ma H. Two new triterpenes from *Euphorbia alatavica*. J Asian Nat Prod Res. 2017;6020:1–8.
19. Gvazava L, Gorgaslidze N, Ganzera M, Skhirtladze A. A new lupane triterpene glycoside from *Euphorbia boissierana* Prokh. Trends Phytochem Res. 2017;1(3):149–52.
20. Wang S, Liang H, Zhao Y, Wang G, Yao H, Kasimu R, et al. New triterpenoids from the latex of *Euphorbia resinifera* Berg . Fitoterapia. 2016;108:33–40.
21. Wang S, Huang C, Sun R, Lu L, Liang H, Gao L. New tirucallane triterpenoids from the dried latex of *Euphorbia resinifera*. Phytochem Lett. 2019;29:220–4.
22. Duong T, Beniddir MA, Genta-jouve G, Nguyen H, Nguyen D, Nguyen T, et al. Further terpenoids from *Euphorbia tirucalli*. Fitoterapia. 2019;135:44–51.
23. Liu T, Liang Q, Xiong N, Dai L, Wang J, Ji X. A new ent-kaurane diterpene from *Euphorbia stracheyi* Boiss. Nat Prod Res. 2017;6419:233–8.
24. Yan S, Li Y, Chen X, Liu D, Chen C, Li R. Diterpenes from the stem bark of *Euphorbia neriifolia* and their in vitro anti-HIV activity. Phytochemistry. 2018;145:40–7.
25. Wang J, Wang Q, Zhen Y, Zhao S, Gao F. Cytotoxic Lathyrane-Type Diterpenes from Seeds of *Euphorbia lathyris*. 2018;66(6):674–7.
26. Durán-Peña MJ, Flores-Giubi ME, Botubol-Ares JM, Escobar-Montaño F, Macías-Sánchez AJ, Echeverri LF, et al. Lathyrane Diterpenes from the Latex of *Euphorbia laurifolia*. Nat Prod Commun. 2017;97(5):8–10.
27. Han C, Peng Y, Wang Y, Huo X, Zhang B, Li D. Cytotoxic *ent*-Abietane-type diterpenoids from the roots of *Euphorbia ebracteolata*. Bioorg Chem. 2018;81:93–7.
28. Bai J, Huang X, Liu Z, Gong C, Li X, Li D. Four new compounds from the roots of

Euphorbia ebracteolata and their inhibitory effect on LPS-induced NO production. Fitoterapia. 2018;125:235-239.

29. Benmerache A, Magid AA, Labed A, Voutquenne-nazabadioko L, Hubert J, Morjani H, et al. Isolation and characterisation of cytotoxic compounds from *Euphorbia clementei* Boiss . Nat Prod Res. 2017;31(18):2091-2098.
30. Jian B, Zhang H, Han C, Liu J. Anti-Cancer Activities of Diterpenoids Derived from *Euphorbia fischeriana* Steud. Molecules. 2018;23(387):1–11.
31. Jin-jun H, Yao S, Zhou Y, Lin F, Lu-ying C, Shuai Y. Anti-proliferation activity of terpenoids isolated from *Euphorbia kansui* in human cancer cells and their structure-activity relationship. Chin J Nat Med. 2017;15(10):766–74.
32. Zhang B, Yin H, Zhang D. Two new *ent*-labdane diterpenes from the roots of *Euphorbia yinshanica*. Chem Nat Compd. 2017;53(2):250–2.
33. Nothias L, Retailleau P, Costa J, Roussi F, Neyts J, Leyssen P, et al. Isolation of Premyrsinane, Myrsinane, and Tigliane Diterpenoids from *Euphorbia pithyusa* using a Chikungunya Virus Cell-Based Assay and Analogue Annotation by Molecular Networking. J Nat Prod. 2017;80:2051–9.
34. Reis MA, André V, Duarte MT, Lage H, Ferreira MU. 12,17-Cyclojatrophane and Jatrophane Constituents of *Euphorbia welwitschii*. J Nat Prod. 2015;78(11):2684–2690;
35. Wang S, Li G, Zhang K, Wang H, Liang H, Huang J, et al. New ingol-type diterpenes from the latex of *Euphorbia resinifera*. J Asian Nat Prod Res. 2019;21(11):1075-1082.
36. Liu J, Yu M, Liao H, Liu T, Tan Y, Liang D. Sesquiterpenes and diterpenes from *Euphorbia thymifolia*. Fitoterapia. 2019;139:104408.
37. Dai L, Liang Q, Liu T, He M, Zhao P, Xu W. A new tigliane-type diterpene from *Euphorbia dracunculoides* Lam. Nat Prod Res. 2016;30(14):1639-45.
38. Kúsz N, Orvos P, Csorba A, Tálosi L, Chaieb M, Hohmann J, et al. Jatrophane diterpenes from *Euphorbia guyoniana* are new potent inhibitors of atrial GIRK channels. Tetrahedron. 2016;72(37):5724-5728;
39. Trimedona N, Pertanian P, Payakumbuh N, Darwis D, Efdi M, Andalas U. Isolation of triterpenoid from stem bark of *Pometia pinnata* , Forst & Forst. J Chem Pharm Res. 2015;7:225–7.
40. Moulisha B, Bikash MN, Partha P, Ashoke G, Sukdeb B, Kanti HP. In vitro Anti-Leishmanial and Anti-Tumour Activities of a Pentacyclic Triterpenoid Compound Isolated from the Fruits of *Dregea volubilis* Benth Asclepiadaceae. Trop J Pharm Res.

2009;8:127–31.

41. Ma X-C, Dong S, Zhang S-Y, Jia N, Ou S-L. Taraxerone triterpene inhibits cancer cell growth by inducing apoptosis in non cells. Bangladesh J Pharmacol. 2016;(11):342–7.
42. Koay YC, Wong KC, Osman H, Eldeen I, Asmawi Zaini M. Chemical Constituents and Biological Activities of *Strobilanthes crispus* L . Rec Nat Prod. 2013;7(1):59–64.
43. Yao X, Ph D, Lu B, Sc B, Lü C, Ph D, et al. Taraxerol Induces Cell Apoptosis through A Mitochondria-Mediated Pathway in HeLa Cells. Cell J. 2017;19(3):512–9.
44. Sharma K, Zafar R. Occurrence of taraxerol and taraxasterol in medicinal plants. Pharmacogn Rev. 2015;9(17):19–24.
45. Thuy TT, Sung T Van, Frank K, Wessjohann L. Triterpenes from the roots of *Codonopsis pilosula*. J Chem. 2008;46:515–20.
46. Hong J, Song Y, Liu Z, Zheng Z, Chen H, Wang S. Anticancer activity of taraxerol acetate in human glioblastoma cells and a mouse xenograft model via induction of autophagy and apoptotic cell death, cell cycle arrest and inhibition of cell migration. Mol Med Rep. 2016;(13):4541–8.
47. Rahman U ur, Durrani S, Ubaidullah, Ali S, Rahman S ur. Anti-pyretic activity of taraxerol acetate. KJMS. 2016;Vol. 9(3486):165–7.
48. Rahman U, Ali S, Khan I, Khan MA, Arif S, Wazir R. Anti-inflammatory activity of taraxerol acetate. J Med Sci. 2016;24(4):4–7.
49. Nyigo VA, Peter X, Faith M, Hamisi MM, Robinson HM, Fouche G. Isolation and identification of euphol and β-sitosterol from the dichloromethane extracts of *Synadenium glaucescens*. J Phytopharm. 2016;5(3):100–4.
50. Rauf A, Uddin G, Khan H, Raza M. Anti-tumour-promoting and thermal-induced protein denaturation inhibitory activities of β-sitosterol and lupeol isolated from *Diospyros lotus* L. Nat Prod Res Former Nat Prod Lett. 2015;30(10):1205-1207.
51. Novotny L, Abdel-hamid ME, Hunakova L. Anticancer potential of β-Sitosterol. Int J Clin Pharmacol Pharmacother. 2017;2:2–5.
52. Dighe SB, Kuchekar BS, Wankhede SB. Analgesic and anti-inflammatory activity of β -sitosterol isolated from leaves of *Oxalis corniculata*. Int J Pharmacol Res. 2016;6(03):109–13.
53. Giang PM, Huynh Nga DT, Hai NX, Tong Son P. Further chemical constituents of *Scoparia dulcis* L. (Scrophulariaceae) originating in Vietnam. J Chem. 2009;47:640–6.
54. Faure R, Emile MG. Application of inverse-detected two-dimensional heteronuclear-correlated nmr spectroscopy to the complete carbon-13 assignment of isomultiflorenyl

acetate. J Nat Prod. 1991;54(6):1564–9.

55. Valente C, Pedro M, R. Ascenso J, M. Abreu P, São José Nascimento M, José U. Ferreira M. Euphopubescenol and Euphopubescene , Two New Jatrophane Polyesters , and Lathyrane-type Diterpenes from *Euphorbia pubescens*. Planta Med. 2004;7:3–8.
56. Nim S, Mónico A, Rawal MK, Duarte N, Prasad R, Pietro A Di, et al. Overcoming Multidrug Resistance in Candida albicans : Macrocyclic Diterpenes from *Euphorbia* Species as Potent Inhibitors of Drug Efflux Pumps. Planta Med. 2016;82:1180–5.
57. Jia Z, Ding Y. New Diterpenoids from *Euphorbia sieboldiana*. Planta Med. 1991;57:569–71.
58. Yu L, Ni T, Gao W, He Y, Wang Y, Cui H, et al. The synthesis and antibacterial activity of pyrazole-fused tricyclic diterpene derivatives. Eur J Med Chem. 2015;90:10–20.
59. Wang H, Liu Y, Zhang J, Xu J, Cui C, Guo Y. 15-O-Acetyl-3-O-benzoylcharaciol and helioscopinolide A , two diterpenes isolated from *Euphorbia helioscopia* suppress microglia activation. Neurosci Lett. 2016;612:149–54.
60. Crespi-perellino N, Garofano L, Arlandini E, Pinciroli V, Danieli B. Identification of New Diterpenoids from *Euphorbia calyptrata* Cell Cultures. J Nat Prod. 1996;59:773–6.
61. Kumar A, Jaitak V. Natural products as multidrug resistance modulators in cancer. Eur J Med Chem. 2019;176:268–91.
62. Borghi D, Baumer L, Ballabio M, Arlandini E. Structure elucidation of helioscopinolides D and E from *Euphorbia calyptrata* cell cultures. J Nat Prod. 1991;54(6):1503–8.
63. Li Y, Yue R, Liu R, Zhang L, Wang M. Secondary Metabolites from the Root of *Aralia echinocaulis* Hand . -Mazz . Rec Nat Prod. 2016;10(5):639–44.
64. Kalantarzadeh M, Mulholland DA, Leij FAAM De, Webber JF. Induced antimicrobial activity in heat-treated woodchips inhibits the activity of the invasive plant pathogen *Phytophthora ramorum*. Plant Pathol. 2019;889–900.
65. Kim KM, Heo DR, Kim Y, Lee J, Kim NS, Bang O. Coniferaldehyde inhibits LPS-induced apoptosis through the PKC α/β II / Nrf-2 / HO-1 dependent pathway in RAW264.7 macrophage cells. Environ Toxicol Pharmacol. 2016;48:85–93.
66. Jeon J, Kwon H, Cho E, Sook K, Yun J, Choon Y, et al. The effect of coniferaldehyde on neurite outgrowth in neuroblastoma. Neurochem Int. 2019;131:104579.